

Stackelberg Games with k -Submodular Function under Distributional Risk-Receptiveness and Robustness

Seonghun Park¹ and Manish Bansal^{*1}

¹*Grado Department of Industrial and Systems Engineering, Virginia Polytechnic Institute and State University, Blacksburg, Virginia, 24061, USA*

June 18, 2024

Abstract

We study submodular optimization in adversarial context, applicable to machine learning problems such as feature selection using data susceptible to uncertainties and attacks. We focus on Stackelberg games between an attacker (or interdictor) and a defender where the attacker aims to minimize the defender’s objective of maximizing a k -submodular function. We allow uncertainties arising from the success of attacks and inherent data noise, and address challenges due to incomplete knowledge of the probability distribution of random parameters. Specifically, we introduce Distributionally Risk-Averse k -Submodular Interdiction Problem (DRA k -SIP) and Distributionally Risk-Receptive k -Submodular Interdiction Problem (DRR k -SIP) along with finitely convergent exact algorithms for solving them. The DRA k -SIP solution allows risk-averse interdictor to develop robust strategies for real-world uncertainties. Conversely, DRR k -SIP solution suggests aggressive tactics for attackers, willing to embrace (distributional) risk to inflict maximum damage, identifying critical vulnerable components, which can be used for the defender’s defensive strategies. The optimal values derived from both DRA k -SIP and DRR k -SIP offer a confidence interval-like range for the expected value of the defender’s objective function, capturing distributional ambiguity. We conduct computational experiments using instances of feature selection and sensor placement problems, and Wisconsin breast cancer data and synthetic data, respectively.

Keywords: k -submodular function, distributionally risk averse optimization, distributionally risk-receptive, feature selection problem, adversarial machine learning

1 Introduction and Motivation

Submodularity is an important concept in the domain of combinatorial optimization as submodular functions encompass various classes of functions, including weighted coverage,

^{*}Corresponding author (bansal@vt.edu)

entropy, and mutual information functions (Krause and Golovin, 2014). Consequently, the submodular functions have found extensive use in machine learning with applications such as feature selection (Liu et al., 2013; Wei et al., 2015), image segmentation (Boykov and Jolly, 2001), data summarization (Lin and Bilmes, 2010), influence maximization (Kempe et al., 2003), and sensor placement (Krause et al., 2008a,b,c). Recently, it has been observed that machine learning models are susceptible to unexpected noise associated to the training or testing data, and to the adversarial attacks where an adversary can inject deteriorated training data, thereby leading to inaccuracies in the output results (Goodfellow et al., 2014). For an example, the feature selection process becomes significantly more complex in adversarial scenarios due to the actions of attackers aiming to degrade model performance through feature removal or label manipulation (Li et al., 2017).

In this paper, we consider Stackelberg games with submodular functions that involve two non-cooperating players: an interdictor (or attacker) and a follower (or defender). The attacker with limited budget aims to minimize the defender’s objective of maximizing a submodular function by interdicting a subset of the ground set. The attacker’s optimal solution identifies the subset of ground set whose disruption would most significantly undermine defender’s possible objective and this approach enables the attacker to prioritize the resources effectively, by targeting the most vulnerable components for maximum disruption. We explore this framework across two distinct problems: the Feature Selection Interdiction Problem (FSIP) and the Weighted Coverage Interdiction Problem (WCIP), both characterized by the defender’s objective function being submodular. In FSIP, the attacker targets specific data features to degrade the model performance and, as a response, a defender selects an optimal subset of remaining features, by maximizing submodular function. Similarly, in WCIP, attacker aims to minimize the defender’s maximum possible coverage by interdicting certain locations, and defender positions sensors at a subset of unattacked locations to achieve possible maximal coverage. This modeling framework can also be used to strategize the most effective interdiction actions aimed at restraining an evader or enemy with an objective of feature selection and sensors placement.

The relevance of submodular function optimization in adversarial settings is underscored. While previous research (Tanınmış and Sinnl, 2022) assumes known input parameters, the unpredictable nature of real-world data introduces additional challenges (He et al., 2019). These factors highlight the needs to develop submodular optimization approaches to effectively address uncertainties in adversarial contexts where the robustness of decisions in the midst of randomness is crucial. In this paper, we introduce stochastic submodular interdiction problems to handle uncertainties in the success of attacks and data associated with the ground set (e.g., uncertain data corresponding to each feature in a feature selection problem). Specifically, the attacker/interdictor aims to remove components (i.e., features or potential sensor locations) of the ground set to minimize the expected value of the defender’s objective function. However, in many applications, the evaluation of expectation is constrained by the limited availability of historical data, which complicates the estimation of true probability distributions associated with uncertain data parameters. To address this additional challenge, we employ distributionally robust optimization (DRO) framework that optimizes objective function for the worst-case probability distribution within a predefined set, known as the ambiguity set (Dupačová, 1987; Scarf et al., 1957). This framework yields a distributionally robust solution for a risk-averse attacker, thereby offering a robust attack-

ing strategy when the interdictor is the main protagonist. From the defender’s perspective, the assumption that the attacker’s strategy is solely risk-averse could lead to a misjudgment of the attacker’s desire for aggressive actions (receptiveness to take risk), potentially leaving the defender unprepared for more risky and impacting tactics. To this end, we introduce distributionally risk-averse submodular interdiction problem (DRA SIP) and a distributionally risk-receptive submodular interdiction problem (DRR SIP). An optimal solution for the DRR SIP emphasizes key vulnerabilities, identifying which elements, if compromised, would most severely degrade their objectives, thereby guiding the development of targeted defensive strategies.

Furthermore, in many practical applications, the challenge often involves selecting multiple disjoint subsets instead of a single subset. For instance, consider the problem where defender aims to maximize area coverage by deploying $k \in \mathbb{Z}_+$ distinct types of sensors, each with a unique range, and are constrained to install at most one sensor for each location. This situation underscores the need for a mathematical model that can address the selection of multiple, distinct subsets to optimize a given objective. To incorporate this feature, we employ k -submodular function (Huber and Kolmogorov, 2012), which reduces to standard submodular function when $k = 1$, as a defender’s objective function in stochastic SIP, DRA SIP and DRR SIP. We denote these generalized problems as stochastic k -SIP, DRA k -SIP and DRR k -SIP, and present exact solution approaches to solve them. This incorporation not only addresses the problem of placing k -types of sensors for maximizing the coverage but also extends applicability of our research to any situation where k -submodular function can be employed (Ohsaka and Yoshida, 2015; Singh et al., 2012).

1.1 Contributions and Organization of the Paper

As per our knowledge, stochastic k -SIP, DRA k -SIP and DRR k -SIP have not been addressed in current literature for any $k \geq 1$ and moreover, deterministic k -SIP has not been studied for $k \geq 2$. We review the literature related to these problems in Section 2. In Section 3, we present necessary background for submodular and k -submodular functions and introduce the formulations of deterministic k -SIP, stochastic k -SIP, DRA k -SIP and DRR k -SIP. Next, in Section 4, we describe exact solution methodologies for solving DRA k -SIP and DRR k -SIP (that subsume both deterministic and stochastic k -SIPs), by introducing families of valid inequalities and embedding them within decomposition-based approaches. In Sections 5 and 6, we present results of our computational experiments and concluding remarks, respectively.

To evaluate the impact of this paper, we use the Wisconsin Breast Cancer Data (Wolberg et al., 1995) for FSIP and obtain optimal solutions for both attacker (interdicted features) and defender (selected features) by solving deterministic, DRA, stochastic, and DRR k -SIPs for $k = 1$. Four Support Vector Classifiers (SVCs) were trained using only the defender-selected features from each problem types and tested against 100 noise-injected scenarios, to estimate the robustness of attacking strategies. Figure 1 illustrates the performance of SVCs, where each dot represents the test accuracy of the SVCs for noise-injected data sets, and the enveloping colored curves represent the frequency of occurrence of these accuracy dots out of the 100 scenarios and two flat lines in the curvature represent the mean (along with mean values) and the median (without mean values). Observe that the test accuracy range for the SVC trained with DRA-SIP solution aligns closely with those trained using

solutions from both deterministic and stochastic (risk-neutral) SIPs, i.e., from 89% to 95%. However, the test accuracy range for the SVC trained with the solution from DRR SIP spans from 82% to 96%, presenting a broader distribution compared to other attacking strategies. This suggests that attacking strategy derived from DRR-SIP has the potential to degrade prediction model more significantly compared to other attacking strategies. In a nutshell, this analysis provides not only bounds on the accuracy for varying levels of risk-appetite (ranging from risk-aversion to risk-receptiveness) of decision makers but also returns most vulnerable features of the data set. (Refer to Section 5.2 for results of computational experiments conducted on randomly generated instances of weighted coverage problem.)

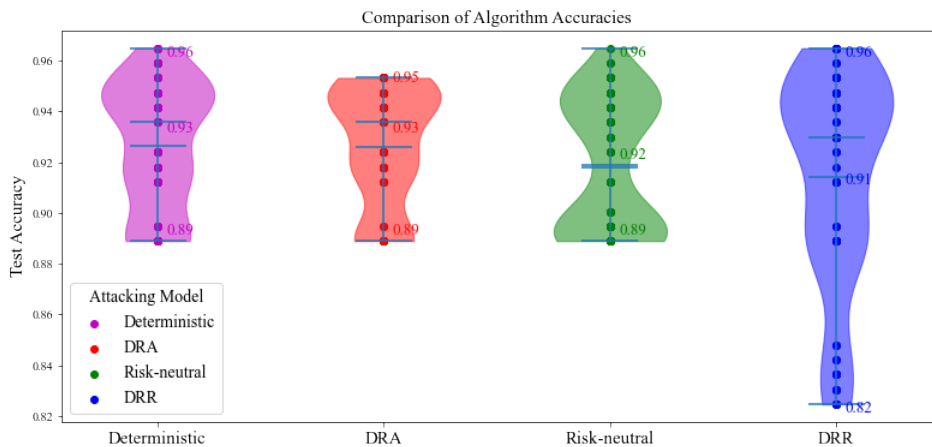


Figure 1: Performance of Support Vector Classifiers (SVCs) on Wisconsin Breast Cancer Data (Wolberg et al., 1995) using defender-selected features provided by different modeling framework

2 Literature Review

In this section, we review the literature related to submodular function, k -submodular function, Stackelberg zero-sum games (also referred as interdiction games), and adversarial machine learning including feature selection problems.

2.1 k -Submodular Functions and Their Applications

Submodular functions have a wide range of applications. Krause and Golovin (2014) provided a comprehensive survey of the applications of submodularity in machine learning. Vohra and Hall (1993) solved maximal covering problem by leveraging submodular objective function. Likewise, Nemhauser et al. (1978) showed that the objective function of the incapacitated facility location problem can be formulated as a monotone submodular function and provided a greedy algorithm with $(1 - 1/e)$ approximation ratio for solving it. In another direction, Wei et al. (2015) introduced framework for unsupervised data subset selection problem by formulating maximum likelihood estimator function of Naïve Bayes classifier and Nearest

Neighbor classifiers as submodular function and selecting the data subset which maximizes this submodular function using the greedy approach. Recently, Kothawade et al. (2022) introduced various submodular information measures for data subset selection with the aim of selecting subsets with desired characteristics.

A generalization of the submodular function, referred to as a k -submodular function, was introduced by Huber and Kolmogorov (2012). As mentioned earlier, it has been widely applied to the applications such as multi-topic influence maximization problem (Rafiey and Yoshida, 2020; Ohsaka and Yoshida, 2015), multi-type sensor placement problem (Ohsaka and Yoshida, 2015; Qian et al., 2017) and information coverage problem (Qian et al., 2017). Acknowledging its practicability, most of the research focus on the methodology to maximize k -submodular functions. Ohsaka and Yoshida (2015) introduced a greedy algorithm for monotone k -submodular function maximization under two types of size constraints: an overall cardinality constraint and individual cardinality constraints for each of the k subsets. Their greedy approach achieved approximation ratios of $1/2$ and $1/3$ for these respective constraints. Expanding upon this, Sakaue (2017) addressed matroid constraints, yielding a $1/2$ -approximation algorithm, while Tang et al. (2022) focused on non-negative monotone k -submodular function maximization under knapsack constraints, attaining an approximation ratio of $(\frac{1}{2} - \frac{1}{2e})$. While the majority of research has been focused on approximation methods, Yu and Küçükyavuz (2021) offered an exact solution approach. They first introduced valid inequality which is the tight upper approximation of the hypograph of any k -submodular function and incorporate them in the delayed constraint generation method for repeatedly refining hypograph of k -submodular function to solve the problem exactly.

2.2 Stackelberg Zero-Sum Games

The attacker-defender dynamics is commonly modeled through Stackelberg zero-sum games. A representative problem of this domain is the Network Interdiction Problem (NIP), (Fulkerson and Harding, 1977; Israeli and Wood, 2002), where an attacker aims to disrupt a network of nodes and arcs, thereby hindering a defender’s (also known as an evader or follower) ability to transport illegal drugs or nuclear materials. The goal of the defender is to either maximize the flow (Wollmer, 1964) or minimize the shortest path (Israeli and Wood, 2002) from source node to destination node, and the interdicator’s aim is to minimize or maximize, respectively, the defender’s objective. Israeli and Wood (1999) introduced stochastic network interdiction problem by incorporating uncertain data parameters defined by random variables with known probability distribution. Readers can refer to Smith and Song (2020) for a comprehensive survey on other variants of NIP. Building on the literature, Kang and Bansal (2023) considered incomplete information of probability distribution associated with uncertain parameters in stochastic NIP, and offered adjustments based on varying level of risk-appetite of decision makers in NIP. In another direction, Park and Bansal (2024) extended beyond the conventional formulations of the defender’s problem as linear or integer programs. They considered a computational geometry problem of placing multiple rectangular camera view-frames to capture areas with maximum threat as defender’s problem. Similarly, Tanınmış and Sinnl (2022) explored a deterministic interdiction game with a monotone 1-submodular function as the defender’s objective and presented a branch-and-cut based exact solution approach for solving this problem.

2.3 Machine Learning in the Presence of Adversarial Attacks

For the sake of completeness of literature review, we briefly review some advances in adversarial machine learning that are relevant for this paper. Kurakin et al. (2016) pointed that machine learning models are susceptible to the adversarial attacks such as intentionally injected malicious input samples or noise. They emphasized the importance of constructing robust models that perform well in various adversarial scenarios. For feature selection problem, Globerson and Roweis (2006) introduced a problem where a subset of features of test instances is interdicted and thereby the support vector machine model trained using labeled train data with all features, can only rely on the subset of features associated with test data for the classification. This led to a game-theoretic min-max problem allowing defender (i.e., data user) to build a model that is resilient to feature interdiction executed by the attacker. Dekel and Shamir (2008) presented a more efficient algorithm for solving the foregoing problem by taking into account the level of importance of each feature. Both studies optimized the objective function based on the labeled training data, thereby relying provided label information. They developed robust models for test samples, where only a subset of the training data features is available, and different features may be interdicted for different test data points. However, they did not account for uncertainty and incomplete information regarding the probability distribution. Additionally, their approach depend on the label information, which can be vulnerable to attacks.

In the domain of Graph Neural Networks, addressing adversarial attack on graph structures has become a critical area of research. Dai et al. (2018) proposed reinforcement learning-based effective attacking strategy by modifying or deleting edges of the graph structure where the model learns to attack the graph from the classifier’s prediction. Xu et al. (2019) also introduced a gradient-based attack method to obstruct the processing of graph structured data by data users, and adversarial learning techniques for graph neural network to build more robust models against such attacks. As per our knowledge, the aforementioned studies do not incorporate the following features: uncertainty in the data, incomplete information of probability distribution, and adjustments based on risk-appetite of a decision maker.

3 k -Submodular Interdiction Problems without and with Uncertainty: Formulations and Applications

In this section, we provide some definitions necessary to introduce formulations of four problems: Deterministic, Stochastic (Risk-Neutral), Distributionally Risk-Averse (DRA), and Risk-Receptive (DRR) k -SIPs. We also present two applications of these formulations, i.e., feature selection interdiction problem and weighted coverage interdiction problem, that we employ for our computational experiments as well.

Definition 3.1 (Submodular function). *Let $N = \{1, \dots, n\}$ be a non-empty finite ground set. A function f is a monotone submodular if for every $A \subseteq B \subseteq N$ and $i \in N \setminus B$, the following holds:*

$$\rho_i(A) = f(A \cup \{i\}) - f(A) \geq f(B \cup \{i\}) - f(B) = \rho_i(B), \quad (1)$$

where $\rho_i(\cdot)$ is a marginal gain of adding element i .

Definition 3.2 (Set of k Disjoint Sets). For $k \geq 1$ and $N = \{1, \dots, n\}$, we denote a set of all k disjoint subsets of N by

$$\mathbb{X}(N, k) = \{(Z_1, \dots, Z_k) : Z_q \subseteq N \text{ for all } q \in \{1, \dots, k\} \text{ and } Z_q \cap Z_{q'} = \emptyset \text{ for } q \neq q'\}.$$

Definition 3.3 (k -Submodular Function). A function $f : \mathbb{X}(N, k) \rightarrow \mathbb{R}$ is a k -submodular function if for any $\mathbf{X} = (X_1, \dots, X_k)$ and $\mathbf{Y} = (Y_1, \dots, Y_k) \in \mathbb{X}(N, k)$, the following holds:

$$f(\mathbf{X}) + f(\mathbf{Y}) \geq f(\mathbf{X} \sqcap \mathbf{Y}) + f(\mathbf{X} \sqcup \mathbf{Y}) \quad (2)$$

where $\mathbf{X} \sqcap \mathbf{Y} = (X_1 \cap Y_1, \dots, X_k \cap Y_k)$ and

$$\mathbf{X} \sqcup \mathbf{Y} = \left\{ (X_i \cup Y_i) \setminus \bigcup_{\substack{q=1 \\ q \neq i}}^k (X_q \cup Y_q), \right\}_{i=1}^k$$

Definition 3.4 (Marginal Gains for k -Submodular Functions). Given $\mathbf{X} \in \mathbb{X}(N, k)$, for any $q \in \{1, \dots, k\}$, $i \in N \setminus \bigcup_{r=1}^k X_r$, the marginal gain of adding i to X_q is defined as

$$\rho_{q,i}(\mathbf{X}) = f(X_1, \dots, X_q \cup \{i\}, \dots, X_k) - f(\mathbf{X}).$$

If function f is k -submodular, then for every $\mathbf{X}, \mathbf{Y} \in \mathbb{X}(N, k)$ such that $X_r \subseteq Y_r$ for all $r \in \{1, \dots, k\}$,

$$\rho_{q,i}(\mathbf{X}) \geq \rho_{q,i}(\mathbf{Y}) \quad \text{for all } i \in N \setminus \bigcup_{r=1}^k Y_r \text{ and } q \in \{1, \dots, k\}.$$

Definition 3.5 (k -Submodular Maximization). Given a set of problem dependent feasible solutions $\mathcal{S} \subseteq \mathbb{X}(N, k)$, the k -submodular maximization problem is defined as:

$$\max\{f(\mathbf{S}) : \mathbf{S} \in \mathcal{S}\}. \quad (3)$$

For any $\mathbf{S} \in \mathbb{X}(N, k)$, we can write $f(\mathbf{S}) = f(\mathbf{s})$ where $\mathbf{s} = (s_1, \dots, s_k) \in \{0, 1\}^{kn}$ and $s_{q,i} = 1$ when $i \in S_q$, and $s_{q,i} = 0$ otherwise for all $q \in \{1, \dots, k\}$ and $i \in N$.

3.1 Formulations for k -SIPs without and with Uncertainty

To illustrate the formulation of the deterministic k -submodular interdiction problem, we consider an example of the weighted coverage interdiction problem. In this problem, an interdicator intends to prevent a defender from installing sensor of type $q \in \{1, \dots, k\}$ at location $i \in N$ by minimizing the defender's objective of maximizing coverage. The interdicator's decision variable $x_{q,i} = 1$ if he decides to block the installation of a type q sensor at sites i and 0 otherwise. In contrast, we denote the defender's decisions by $\mathbf{S} = (S_1, \dots, S_k) \subseteq \mathbb{X}(N, k)$ where S_q represents a set of locations where the defender choose to place type $q \in \{1, \dots, k\}$ sensors. We assume that both players are subject to budget limitations for each sensor type

$q \in \{1, \dots, k\}$, denoted as A_q and D_q for the interdicator and defender, respectively. We formulate the deterministic k -submodular interdiction problem as:

Deterministic k -SIP

$$\min_{\mathbf{x} \in \mathcal{X}} \Phi_D(\mathbf{x}) \quad (4a)$$

$$\text{where } \mathcal{X} := \left\{ \mathbf{x} \in \{0, 1\}^{kn} : \sum_{i=1}^n x_{q,i} \leq A_q, \forall q \in \{1, \dots, k\}, \sum_{q=1}^k x_{q,i} \leq 1, \forall i \in N \right\}, \quad (4b)$$

$$\Phi_D(\mathbf{x}) := \max \left\{ f(\mathbf{S}) : \mathbf{S} \in \mathbb{X}(N, k), s_{q,i} \leq 1 - x_{q,i}, \forall q \in \{1, \dots, k\}, \forall i \in N, \quad (4c)$$

$$\left. \sum_{i=1}^n s_{q,i} \leq D_q, \forall q \in \{1, \dots, k\} \right\}. \quad (4d)$$

In (4b), first constraint enforces the budget limits for the interdicator for each $q \in \{1, \dots, k\}$, and the second constraint ensures that the interdicator selects k disjoint subsets, i.e., for each location $i \in N$, an interdicator can block the installation of at most one type of sensor $q \in \{1, \dots, k\}$. The constraint in (4c) indicates that the defender cannot place sensor type $q \in \{1, \dots, k\}$ at location $i \in N$ if it has been blocked by the attacker's solution \mathbf{x} . Constraint(4d) enforces defender's budget limits for each $q \in \{1, \dots, k\}$.

We also present formulations for problem (4) with two types of uncertainties. We represent the uncertainty associated with the success of attack vector and noise in the data set using random variables $\xi \in \{0, 1\}^n$ and \mathcal{D} with m samples and n number of features, respectively. Let $\Omega := \{\omega_1, \dots, \omega_{|\Omega|}\}$ be a finite set of possible realizations of (ξ, \mathcal{D}) and each realization $(\xi^\omega, \mathcal{D}^\omega)$ occurs with probability p_ω . Contrary to the initial assumption in problem (4) that every attack by an attacker is successful, we assume that the attack on location $i \in N$ for type $q = \{1, \dots, k\}$ is successful if and only if the condition $\xi_i^\omega \cdot x_{q,i} = 1$ is satisfied. Moreover, due to uncertain data set \mathcal{D} , function value $f(\cdot)$ varies across scenarios $\omega \in \Omega$, which we represent as $f^\omega(\cdot)$. After observing the attacker's solution $\mathbf{x} \in \mathcal{X}$ and a realization of uncertainties $\omega \in \Omega$, the defender selects subset of available items, denoted by \mathbf{S}^ω , to maximize its k -submodular function. For $\omega \in \Omega$, the defender's problem is defined as

$$Q_\omega(\mathbf{x}, \xi^\omega) := \max \left\{ f^\omega(\mathbf{S}^\omega) : \mathbf{S}^\omega \in \mathbb{X}(N, k), \quad (5a)$$

$$s_{q,i}^\omega \leq 1 - x_{q,i} \xi_i^\omega, \forall q \in \{1, \dots, k\} \text{ and } i \in N, \quad (5b)$$

$$\left. \sum_{i=1}^n s_{q,i}^\omega \leq D_q, \forall q \in \{1, \dots, k\} \right\}. \quad (5c)$$

If probability distribution P associated with random parameters is known, we get **Stochastic (Risk-Neutral) k -SIP**

$$\min_{\mathbf{x} \in \mathcal{X}} \Phi_N(\mathbf{x}) := \mathbb{E}_P[Q_\omega(\mathbf{x}, \xi^\omega)], \quad (6)$$

where $\mathbb{E}_P[\cdot]$ is an expectation operator.

When complete information of the probability distribution P is not known and it belongs to a predefined ambiguity set \mathfrak{P} , we formulate Distributionally Risk-Receptive k -Submodular Interdiction Problem (DRR k -SIP) and Distributionally Risk Averse k -Submodular Interdiction Problem (DRA k -SIP) with the predefined ambiguity set \mathfrak{P} as follows.

DRR k -SIP

$$\min_{\mathbf{x} \in \mathcal{X}} \left\{ \Phi_R(\mathbf{x}) := \min_{P \in \mathfrak{P}} \mathbb{E}_P[Q_\omega(\mathbf{x}, \xi^\omega)] \right\} \quad (7)$$

DRA k -SIP

$$\min_{\mathbf{x} \in \mathcal{X}} \left\{ \Phi_A(\mathbf{x}) := \max_{P \in \mathfrak{P}} \mathbb{E}_P[Q_\omega(\mathbf{x}, \xi^\omega)] \right\} \quad (8)$$

where the inner minimization and maximization with respect to the ambiguity set handle the risk-receptiveness and risk-aversion of the interdictor by selecting best-case and worst-case distributions, respectively. In case $|\mathfrak{P}| = 1$, formulations (7) and (8) reduce to (6). Also, when $|\Omega| = 1$, formulations (6), (7), and (8) reduce to (4).

3.2 Applications of k -SIPs

3.2.1 Feature Selection Interdiction Problem: An Application of 1-SIP

Feature selection is a fundamental problem in machine learning, where the goal is to identify a subset of relevant features that contribute most significantly to the predictive performance of a machine learning model. This process not only enhances model interpretability but also improves efficiency by reducing dimensionality and mitigating overfitting issues. Within this context, this paper addresses a specific challenge associated to the feature selection problem in the presence of an adversary. Specifically, data sets are often compromised through targeted attacks on specific features, thereby impacting the performance of predictive models employed by defenders. As a response, defenders select a subset of unaffected features to train their models, aiming to reduce the impact of these attacks. Submodular functions are employed to assist in this feature selection process, a method proven effective by Liu et al. (2013); Lin and Bilmes (2009) for choosing subset of features. This strategy is centered around the use of selected features for model training and focusing on maintaining model efficacy rather than enhancing performance directly.

Mathematically, FSIP is defined as follows. Given a data set \mathcal{D} with m data samples each containing n features (represented by an m by n matrix). Let $w_{i,j} (\geq 0)$ be a similarity between feature i and j . Then, function $f : 2^N \rightarrow \mathbb{R}$ defined as

$$f(S) = \sum_{i \in N} \max_{j \in S} w_{i,j}$$

is a monotone submodular function (Liu et al., 2013). This function evaluates a given set $S \in N$ by selecting, for each $i \in N$, a feature $j \in S$ that has the highest similarity to i as given by $w_{i,j}$, and then aggregating these values. Using this function, we solve problems (6), (7), and (8) and obtain optimal solutions for an attacker and defender. For details on the experimental setup and computational results, please refer to section 5.1.

3.2.2 Weighted Sensor Coverage Interdiction Problem as k -SIP

Consider a set $N = \{1, \dots, n\}$ of potential sites for installation of sensors that are of k different types depending on their monitoring ranges. Let $\mu_{i,q}$ be the reward obtained by covering site $i \in N$ using sensor type $q \in \{1, \dots, k\}$. However, only one sensor can be placed at each site, and at most D_q sensors of type $q \in \{1, \dots, k\}$ can be installed. Let $\mathbf{S} = (S_1, S_2, \dots, S_k) \in \mathbb{X}(N, k)$ denotes a feasible sensor placement strategy with S_q representing the set of locations where type q sensors are placed. Consequently, we can compute the total reward by introducing a k -submodular function $f : \mathbb{X}(N, k) \rightarrow \mathbb{R}$, i.e.,

$$f(\mathbf{S}) = \sum_{i \in N} \max_{q \in C_i} \mu_{i,q}$$

where $C_i \subseteq \{1, \dots, k\}$ is the set of sensor types covering site i . Again, using this function, formulations (6), (8), and (7) lead to weighted sensor coverage interdiction problem under uncertainty. In Section 5.2, we describe the experimental setup and results in details.

4 Solution Methodologies: Valid Inequalities and Algorithms

We present valid inequalities for deterministic, DRA k -SIP and DRR k -SIP in Section 4.1, and decomposition-based exact approaches for solving DRA k -SIP and DRR k -SIP in Section 4.2. Specifically, we introduce tight lower approximations for the objective functions of problems (4), (6), (7) and (8) using affine functions that lead to inequalities, which are referred to as valid inequalities (or cutting planes). These inequalities are used to iteratively refine the lower bounds of the objective functions within a decomposition framework, thereby ensuring a global optimal solution (4.2). Note that these objective functions $\Phi_D(\mathbf{x})$, $\Phi_{RN}(\mathbf{x})$, $\Phi_{RR}(\mathbf{x})$, and $\Phi_{RA}(\mathbf{x})$ are non-convex, non-concave, and non-submodular. This complicates the application of known optimization techniques such as gradient methods for optimizing them.

4.1 Valid Inequalities

The term ‘‘valid’’ in valid inequality implies that all feasible solutions satisfy this inequality and hence, the inequality is valid. In the following theorems, we provide these inequalities and for the sake of ease for a reader, all validity proofs are provided in Section 4.3.

Theorem 1. *Given an attacker’s solution $\hat{\mathbf{x}}$ and associated defender’s optimal solution $\hat{\mathbf{S}}$, i.e., $\Phi_D(\hat{\mathbf{x}}) = f(\hat{\mathbf{S}})$ in Formulation (4), the following inequality is valid for all $\mathbf{x} \in \mathcal{X}$:*

$$\Phi_D(\mathbf{x}) \geq \Phi_D(\hat{\mathbf{x}}) - \sum_{q=1}^k \sum_{i \in \hat{S}_q} \rho_{q,i}(\emptyset) x_{q,i} \quad (9)$$

where $\rho_{q,i}(\emptyset)$ is the marginal gain of adding item i to q^{th} empty set in \emptyset , where \emptyset is the tuple consisting of k empty sets.

Theorem 2. Given an attacker's solution $\hat{\mathbf{x}}$ and associated defender's solution in Formulation (4), denoted by $\hat{\mathbf{S}} = (\hat{S}_1, \dots, \hat{S}_k)$ with an arbitrary permutation of elements in $\hat{S}_q := \{i_{q,1}, \dots, i_{q,T_q}\}$ for $q \in \{1, \dots, k\}$. The following inequality is valid for problem (4) for any $\mathbf{x} \in \mathcal{X}$ and it dominates inequality (9), i.e., it provides a tighter lower bound approximation in comparison to (9):

$$\Phi_D(\mathbf{x}) \geq \Phi_D(\hat{\mathbf{x}}) - \sum_{q=1}^k \sum_{t=1}^{T_q} \rho_{q,i_{q,t}}(\hat{\mathbf{S}}_{q,(t)}) x_{q,i_{q,t}}, \quad (10)$$

where $\hat{\mathbf{S}}_{q,(t)} = (\hat{S}_1, \dots, \hat{S}'_{q,(t)}, \emptyset, \dots, \emptyset)$ such that $\hat{S}'_{q,(t)} = \{i_{q,1}, \dots, i_{q,t-1}\}$ for $2 \leq t \leq T_q$ and $\hat{\mathbf{S}}_{1,(1)} = \emptyset$.

Theorem 3. Given an attacker's solution $\hat{\mathbf{x}}$ and associated defender's optimal solutions $\{\hat{\mathbf{S}}^\omega\}_{\omega \in \Omega}$ in formulation (6). The following inequality is valid for all $\mathbf{x} \in \mathcal{X}$:

$$\Phi_N(\mathbf{x}) \geq \Phi_N(\hat{\mathbf{x}}) - \sum_{q=1}^k \sum_{\omega \in \Omega} \sum_{t=1}^{|\hat{S}_q^\omega|} \bar{p}_\omega \rho_{q,i_{q,t}^\omega}(\hat{\mathbf{S}}_{q,(t)}^\omega) \xi_{i_{q,t}^\omega}^\omega x_{q,i_{q,t}^\omega}, \quad (11)$$

where $\{\bar{p}_\omega\}_\omega \in \mathfrak{P}$ in the case where $|\mathfrak{P}| = 1$, and $\hat{\mathbf{S}}_{q,(t)}^\omega$ is defined similar to $\hat{\mathbf{S}}_{q,(t)}$ in Theorem 2.

Theorem 4. Given an attacker's solution $\hat{\mathbf{x}}$ and associated defender's optimal solution $\{\hat{\mathbf{S}}^\omega\}_{\omega \in \Omega}$ in formulation (7), the following inequality is valid for all $\mathbf{x} \in \mathcal{X}$:

$$\Phi_R(\mathbf{x}) \geq \Phi_R(\hat{\mathbf{x}}) - \sum_{q=1}^k \sum_{i \in N} \left(\max_{P \in \mathfrak{P}} \sum_{\omega \in \Omega} p_\omega \rho_{q,i}^\omega(\emptyset) \hat{y}_{q,i}^\omega \right) \xi_i^\omega x_{q,i}, \quad (12)$$

where for $i \in N$ and $q \in \{1, \dots, k\}$,

$$\hat{y}_{q,i}^\omega = \begin{cases} 1 & \text{if } i \in \hat{S}_q^\omega, \\ 0 & \text{otherwise.} \end{cases}$$

Theorem 5. Given an attacker's solution $\hat{\mathbf{x}}$ and associated defender's optimal solutions $\{\hat{\mathbf{S}}^\omega\}_{\omega \in \Omega}$ in formulation (8). Then, the following inequality is valid for all $\mathbf{x} \in \mathcal{X}$:

$$\Phi_A(\mathbf{x}) \geq \Phi_A(\hat{\mathbf{x}}) - \sum_{q=1}^k \sum_{\omega \in \Omega} \sum_{t=1}^{|\hat{S}_q^\omega|} \hat{p}_\omega \rho_{q,i_{q,t}^\omega}(\hat{\mathbf{S}}_{q,(t)}^\omega) \xi_{i_{q,t}^\omega}^\omega x_{q,i_{q,t}^\omega}, \quad (13)$$

where $\{\hat{p}_\omega\}_{\omega \in \Omega} \in \arg \max_{P \in \mathfrak{P}} \sum_{\omega \in \Omega} p_\omega f^\omega(\hat{\mathbf{S}}^\omega)$ and $\hat{\mathbf{S}}_{q,(t)}^\omega$ is defined similar to $\hat{\mathbf{S}}_{q,(t)}$ in Theorem 2.

Observation 6. Inequalities (10), (11), (12), and (13) are tight (hold at equality) for $\mathbf{x} = \hat{\mathbf{x}}$.

4.2 Decomposition Algorithms for DRR and DRA k -SIPs

Since formulations (4) and (6) are special cases of DRR k -SIP, i.e., (7), we present decomposition algorithm for the latter to avoid repetition. Our decomposition algorithm incorporates inequalities (12) to refine the lower bound for problem (7) during each iteration, as detailed in Algorithm 1. The algorithm begins with an initialization stage where the iteration counter $L = 1$, the upper bound $\theta_{dr}^{ub} \leftarrow \infty$, the lower bound $\theta_{dr}^{lb} \leftarrow -\infty$, and an initial feasible solution $\hat{\mathbf{x}}^1$ is selected from the set \mathcal{X} . In each iteration $L \geq 1$, we set $\hat{\mathbf{x}}$ to $\hat{\mathbf{x}}^L$ and solve the defender's problem for every scenario $\omega \in \Omega$, as outlined in Line 4, to obtain $f^\omega(\hat{\mathbf{S}}^\omega)$. Subsequently, in lines 6 and 7, we obtain an extremal optimal probability distribution by solving distribution separation problem:

$$\{\hat{p}_\omega\}_{\omega \in \Omega} \in \arg \min_{P \in \mathfrak{P}} \sum_{\omega \in \Omega} p_\omega f^\omega(\hat{\mathbf{S}}^\omega)$$

and then compute $\Phi_R(\hat{\mathbf{x}}) = \sum_{\omega \in \Omega} \hat{p}_\omega f^\omega(\hat{\mathbf{S}}^\omega)$. If $\Phi_R(\hat{\mathbf{x}})$ is smaller than the current upper bound θ_{dr}^{ub} , we update θ_{dr}^{ub} to the value of $\Phi_R(\hat{\mathbf{x}})$ and the best known solution $\hat{\mathbf{x}}^*$ to $\hat{\mathbf{x}}$. Subsequently, we derive and add inequality (12) to a lower bound approximation model from the previous iteration, \mathcal{M}_{DRR}^{L-1} , obtaining \mathcal{M}_{DRR}^L :

$$\theta_{dr}^{lb} := \min_{\mathbf{x} \in \mathcal{X}} \eta \tag{14}$$

$$\text{s.t. } \eta \geq \Phi_R(\hat{\mathbf{x}}) - \sum_{q=1}^k \sum_{i \in N} \left(\max_{P \in \mathfrak{P}} \sum_{\omega \in \Omega} p_\omega \rho_{q,i}^\omega(\boldsymbol{\theta}) \hat{y}_{q,i}^\omega \right) \xi_i^\omega x_{q,i} \tag{15}$$

for $\hat{\mathbf{x}} \in \{\hat{\mathbf{x}}^1, \dots, \hat{\mathbf{x}}^L\}$

which is a tighter lower bound approximation. We solve \mathcal{M}_{DRR}^L , $L \geq 1$, in Line 12 to get an optimal solution $(\eta^{L+1}, \hat{\mathbf{x}}^{L+1})$ and update the best-known lower bound θ_{dr}^{lb} to η^{L+1} . We terminate the algorithm when the optimality gap $(\theta_{dr}^{ub} - \theta_{dr}^{lb})$ lies within a predetermined threshold ϵ .

Theorem 7. *Algorithm 1 solves DRR k -SIP to global optimality in finite iterations if distribution separation problem, line 6 in Algorithm 1, can be solved in finite iterations.*

Proof. Refer to Section 4.3. □

Remark 8. Algorithms for DRA, Deterministic, and Risk-Neutral k -SIP. *Algorithm 1 with inequalities (10),(11) and (13) in Line 11 provide an exact algorithm for solving problem (4), (6) and (8) respectively.*

4.3 Proof of Theorems 1 - 5 and Theorem 7

Lemma 9 (Yu and Küçükyavuz (2021)). *Let f be a monotone k -submodular function. For any $\mathbf{Y}, \mathbf{Z} \in \mathbb{X}(N, k)$, the following inequality holds:*

$$f(\mathbf{Y}) \leq f(\mathbf{Z}) + \sum_{q=1}^k \sum_{i \in Y_q \setminus \bigcup_{r=1}^k Z_r} \rho_{q,i}(\mathbf{Z}) + \sum_{q=1}^k \sum_{p \in \{1, \dots, k\} \setminus \{q\}} \sum_{i \in Y_q \cap Z_p} \rho_{q,i}(\boldsymbol{\theta}). \tag{16}$$

Algorithm 1 Decomposition Method for the DRR k -SIP (7)

- 1: Let $L \leftarrow 1$, $\theta_{dr}^{lb} \leftarrow -\infty$, $\theta_{dr}^{ub} \leftarrow \infty$, $\hat{\mathbf{x}} \leftarrow \hat{\mathbf{x}}^1 \in \mathcal{X}$;
- 2: **while** $\theta_{dr}^{ub} - \theta_{dr}^{lb} > \epsilon$ **do**
- 3: **for** $\omega \in \Omega$ **do**
- 4: Solve subproblem to get $f^\omega(\hat{\mathbf{S}}^\omega)$;
- 5: **end for**
- 6: Compute $\{\hat{p}\}_{\omega \in \Omega} \in \arg \min_{P \in \mathfrak{P}} \sum_{\omega \in \Omega} p_\omega f^\omega(\hat{\mathbf{S}}^\omega)$;
- 7: Obtain $\Phi_R(\hat{\mathbf{x}}) = \sum_{\omega \in \Omega} \hat{p}_\omega f^\omega(\hat{\mathbf{S}}^\omega)$;
- 8: **if** $\theta_{dr}^{ub} > \Phi_R(\hat{\mathbf{x}})$ **then**
- 9: $\theta_{dr}^{ub} \leftarrow \Phi_R(\hat{\mathbf{x}})$ and $\hat{\mathbf{x}}^* \leftarrow \hat{\mathbf{x}}$;
- 10: **end if**
- 11: Add the following inequality in \mathcal{M}_{DRR}^{L-1} to get \mathcal{M}_{DRR}^L :

$$\eta \geq \Phi_R(\hat{\mathbf{x}}) - \sum_{q=1}^k \sum_{i \in N} \left(\max_{P \in \mathfrak{P}} \sum_{\omega \in \Omega} p_\omega \rho_{q,i}^\omega(\emptyset) \hat{y}_{q,i}^\omega \right) \xi_i^\omega x_{q,i};$$

- 12: Solve \mathcal{M}_{DRR}^L to get optimal solution $(\eta^{L+1}, \hat{\mathbf{x}}^{L+1})$;
 - 13: Update the lower bound $\theta_{dr}^{lb} \leftarrow \eta^{L+1}$ and $\hat{\mathbf{x}} \leftarrow \hat{\mathbf{x}}^{L+1}$;
 - 14: $L \leftarrow L + 1$;
 - 15: **end while**
 - 16: **Return:** Optimal Solution Value θ_{dr}^{ub} and Optimal Solution $\hat{\mathbf{x}}^*$.
-

Proof of Theorem 1. For a feasible attacker's solution $\mathbf{x} = (x_1, \dots, x_k)$, let $N_{\mathbf{x}} = \cup_{q=1}^k N_{x_q}$ be the set of items interdicted by \mathbf{x} where $N_{x_q} = \{i \in N : x_{q,i} = 1\}$ for $q \in \{1, \dots, k\}$. We define $\mathbf{S} = (S_1, \dots, S_k)$, where $S_q = \hat{S}_q \setminus N_{x_q}$ for $q \in \{1, \dots, k\}$. From the definition, it follows that S_q is a subset of \hat{S}_q , and $\sum_{i=1}^n s_{q,i} \leq \sum_{i=1}^n \hat{s}_{q,i} \leq D_q$ holds. Therefore, \mathbf{S} is a feasible defender's solution for the attacker's solution \mathbf{x} . Subsequently, referring to (16), we derive the following:

$$f(\hat{\mathbf{S}}) \leq f(\mathbf{S}) + \sum_{q=1}^k \sum_{i \in \hat{S}_q \setminus \cup_{r=1}^k S_r} \rho_{q,i}(\mathbf{S}) + \sum_{q=1}^k \sum_{p \in \{1, \dots, k\} \setminus \{q\}} \sum_{i \in \hat{S}_q \cap S_p} \rho_{q,i}(\emptyset) \quad (17)$$

$$= f(\mathbf{S}) + \sum_{q=1}^k \sum_{i \in \hat{S}_q \setminus \cup_{r=1}^k S_r} \rho_{q,i}(\mathbf{S}) \quad (18)$$

$$= f(\mathbf{S}) + \sum_{q=1}^k \sum_{i \in \hat{S}_q} \rho_{q,i}(\mathbf{S}) x_{q,i} \quad (19)$$

$$\leq f(\mathbf{S}) + \sum_{q=1}^k \sum_{i \in \hat{S}_q} \rho_{q,i}(\emptyset) x_{q,i}. \quad (20)$$

For any $p, q \in \{1, \dots, k\}$ with $p \neq q$, $\hat{S}_q \cap \hat{S}_p = \emptyset$, and since $S_p \subseteq \hat{S}_p$, equality (18) holds. Similarly, we know that $\hat{S}_q \setminus \bigcup_{r=1}^k S_r = \hat{S}_q \setminus S_q$ and for $i \in S_q$, $x_{q,i} = 0$, thereby (19) holds. Finally, inequality (20) is established from the diminishing return property of the monotone k -submodular function. Thus, we have

$$\Phi_D(\mathbf{x}) \geq f(\mathbf{S}) \geq f(\hat{\mathbf{S}}) - \sum_{q=1}^k \sum_{i \in \hat{S}_q} \rho_{q,i}(\emptyset) x_{q,i} = \Psi(\hat{\mathbf{x}}) - \sum_{q=1}^k \sum_{i \in \hat{S}_q} \rho_{q,i}(\emptyset) x_{q,i}. \quad (21)$$

■

Proof of Theorem 2. For an attacker's solution \mathbf{x} , let $S_q = \hat{S}_q \setminus N_{x_q}$ and $\mathbf{S}_{q,(t)} = (S_1, \dots, S'_{q,(t)}, \emptyset, \dots, \emptyset)$ where $S'_{q,(t)} = \hat{S}'_{q,(t)} \setminus N_{x_q}$ for $2 \leq t \leq T_q$ and $q \in \{1, \dots, k\}$. From the feasibility of \mathbf{S} for \mathbf{x} , the following holds:

$$\begin{aligned} \Phi_D(\mathbf{x}) \geq f(\mathbf{S}) &= \rho_{1,i_{1,1}}(\mathbf{S}_{1,(1)})(1 - x_{1,i_{1,1}}) + \dots + \rho_{1,i_{1,T_1}}(\mathbf{S}_{1,(T_1)})(1 - x_{1,i_{1,T_1}}) \\ &\quad + \rho_{2,i_{2,1}}(\mathbf{S}_{2,(1)})(1 - x_{2,i_{2,1}}) + \dots + \rho_{2,i_{1,T_2}}(\mathbf{S}_{2,(T_2)})(1 - x_{2,i_{2,T_2}}) \\ &\quad \vdots \\ &\quad + \rho_{k,i_{k,1}}(\mathbf{S}_{k,(1)})(1 - x_{k,i_{k,1}}) + \dots + \rho_{k,i_{1,T_k}}(\mathbf{S}_{k,(T_k)})(1 - x_{k,i_{k,T_k}}) \\ &= \sum_{q=1}^k \sum_{t=1}^{T_q} \rho_{q,i_{q,t}}(\mathbf{S}_{q,(t)})(1 - x_{q,i_{q,t}}) \\ &\geq \sum_{q=1}^k \sum_{t=1}^{T_q} \rho_{q,i_{q,t}}(\hat{\mathbf{S}}_{q,(t)})(1 - x_{q,i_{q,t}}) \end{aligned} \quad (22)$$

$$= \Phi_D(\hat{\mathbf{x}}) - \sum_{q=1}^k \sum_{t=1}^{T_q} \rho_{q,i_{q,t}}(\hat{\mathbf{S}}_{q,(t)}) x_{q,i_{q,t}}. \quad (23)$$

From the definition of $\mathbf{S}_{q,(t)}$, $S_q \subseteq \hat{S}_q$ and $S'_{q,(t)} \subseteq \hat{S}'_{q,(t)}$ holds for all $q \in \{1, \dots, k\}$ and $t \in \{1, \dots, T_q\}$ and thereby, inequality (22) holds from the diminishing return property of k -submodular function. It is worth to note that this inequality dominates inequality (9) since $\rho_{q,i_{q,t}}(\hat{\mathbf{S}}_{q,(t)}) \geq \rho_{q,i_{q,t}}(\emptyset)$ for all $t \in \{1, \dots, T_q\}$ for $q \in \{1, \dots, k\}$. ■

Proof of Theorem 3. The proof follows the same arguments as those of Theorem 4 and Theorem 5 with a singleton ambiguity set, i.e., $|\mathfrak{P}| = 1$. ■

Proof of Theorem 4. Given $\tilde{\mathbf{x}} \in \mathcal{X}$, let $\{\tilde{\mathbf{S}}^\omega\}_{\omega \in \Omega}$ be an optimal defender's solution, and $\{\tilde{p}_\omega\}_{\omega \in \Omega}$ be an associated extremal probability distribution, i.e.,

$$\{\tilde{p}_\omega\}_{\omega \in \Omega} \in \arg \min_{P \in \mathfrak{P}} \sum_{\omega \in \Omega} p_\omega f^\omega(\tilde{\mathbf{S}}^\omega).$$

Additionally, for $\omega \in \Omega$, define $N_{\tilde{\mathbf{x}}}^\omega = \bigcup_{q=1}^k N_{\tilde{x}_q}^\omega$ as the set of items interdicted by the attacker's solution $\tilde{\mathbf{x}}$, where $N_{\tilde{x}_q}^\omega = \{i \in N : \tilde{x}_{q,i} \cdot \xi_i^\omega = 1\}$ for $q \in \{1, \dots, k\}$. For $\omega \in \Omega$, we define

$\{\bar{\mathbf{S}}^\omega\}_{\omega \in \Omega} = (\bar{S}_1^\omega, \dots, \bar{S}_q^\omega)$ where $\bar{S}_q^\omega = \hat{S}_q^\omega \setminus N_{\tilde{x}_q}^\omega$ for all $q \in \{1, \dots, k\}$, $\omega \in \Omega$. This ensures that $\{\bar{\mathbf{S}}^\omega\}_{\omega \in \Omega}$ is a feasible defender's solution for the given $\tilde{\mathbf{x}}$. Then,

$$\begin{aligned} \Phi_R(\tilde{\mathbf{x}}) &= \sum_{\omega \in \Omega} \tilde{p}_\omega f^\omega(\tilde{\mathbf{S}}^\omega) \\ &\geq \sum_{\omega \in \Omega} \tilde{p}_\omega f^\omega(\bar{\mathbf{S}}^\omega) \end{aligned} \quad (24a)$$

$$\geq \sum_{\omega \in \Omega} \tilde{p}_\omega \left(f^\omega(\hat{\mathbf{S}}^\omega) - \sum_{q=1}^k \sum_{i \in \hat{S}_q^\omega} \rho_{q,i}^\omega(\boldsymbol{\theta}) \xi_i^\omega \tilde{x}_{q,i} \right) \quad (24b)$$

$$\geq \Phi_R(\hat{\mathbf{x}}) - \sum_{q=1}^k \sum_{\omega \in \Omega} \sum_{i \in \hat{S}_q^\omega} \tilde{p}_\omega \rho_{q,i}^\omega(\boldsymbol{\theta}) \xi_i^\omega \tilde{x}_{q,i} \quad (24c)$$

$$= \Phi_R(\hat{\mathbf{x}}) - \sum_{q=1}^k \sum_{i \in N} \sum_{\omega \in \Omega} \tilde{p}_\omega \rho_{q,i}^\omega(\boldsymbol{\theta}) \hat{y}_{q,i}^\omega \xi_i^\omega \tilde{x}_{q,i} \quad (24d)$$

$$\geq \Phi_R(\hat{\mathbf{x}}) - \sum_{q=1}^k \sum_{i \in N} \left(\max_{P \in \mathfrak{P}} \sum_{\omega \in \Omega} p_\omega \rho_{q,i}^\omega(\boldsymbol{\theta}) \hat{y}_{q,i}^\omega \right) \xi_i^\omega \tilde{x}_{q,i}. \quad (24e)$$

Inequality (24a) holds from the feasibility of set $\{\bar{\mathbf{S}}^\omega\}_{\omega \in \Omega}$ for the attacker's solution $\tilde{\mathbf{x}}$ and inequality (24b) follows from (25). Since $\Phi_R(\hat{\mathbf{x}}) = \min_{P \in \mathfrak{P}} \mathbb{E}_P[Q_\omega(\hat{\mathbf{x}}, \xi^\omega)]$, inequality (24c) holds. Also, from the definition of $\hat{y}_{q,i}^\omega$, inequality (24d) holds. Finally, inequality (24e) holds because $\rho_{q,i}^\omega(\boldsymbol{\theta})$, $\hat{y}_{q,i}^\omega$, ξ_i^ω and $\tilde{x}_{q,i}$ are non-negative for all $q \in \{1, \dots, k\}$ and $i \in N$ and $\{\tilde{p}_\omega\}_{\omega \in \Omega}$ is a feasible solution for the maximization problem in inequality (24e). ■

Proof of Theorem 5. For any feasible attacker's solution \mathbf{x} , define $\bar{\mathbf{S}}^\omega = (\bar{S}_1^\omega, \dots, \bar{S}_q^\omega)$ where $\bar{S}_q^\omega = \hat{S}_q^\omega \setminus N_{x_q}^\omega$ for all $q \in \{1, \dots, k\}$ and $\omega \in \Omega$. From the definition, $\{\bar{\mathbf{S}}^\omega\}_{\omega \in \Omega}$ is a feasible defender's solution for the given \mathbf{x} . Referring to (21), the following holds for all $\omega \in \Omega$:

$$f^\omega(\bar{\mathbf{S}}^\omega) \geq f^\omega(\hat{\mathbf{S}}^\omega) - \sum_{q=1}^k \sum_{i \in \hat{S}_q^\omega} \rho_{q,i}^\omega(\boldsymbol{\theta}) \xi_i^\omega x_{q,i}. \quad (25)$$

Moreover, from (22), the following inequality holds for all $\omega \in \Omega$:

$$f^\omega(\bar{\mathbf{S}}^\omega) \geq f^\omega(\hat{\mathbf{S}}^\omega) - \sum_{q=1}^k \sum_{t=1}^{T_q^\omega} \rho_{q,i_{q,t}^\omega}^\omega(\hat{\mathbf{S}}_{q,(t)}^\omega) \xi_{i_{q,t}^\omega}^\omega x_{q,i_{q,t}^\omega}. \quad (26)$$

Let $\{\bar{p}_\omega\}_{\omega \in \Omega} \in \arg \max_{P \in \mathfrak{P}} \sum_{\omega \in \Omega} p_\omega f(\bar{\mathbf{S}}^\omega)$. Then,

$$\Phi_A(\mathbf{x}) \geq \sum_{\omega \in \Omega} \bar{p}_\omega f^\omega(\bar{\mathbf{S}}^\omega) \quad (27a)$$

$$\geq \sum_{\omega \in \Omega} \hat{p}_\omega f^\omega(\bar{\mathbf{S}}^\omega) \quad (27b)$$

$$\geq \sum_{\omega \in \Omega} \hat{p}_\omega \left(f^\omega(\hat{\mathbf{S}}^\omega) - \sum_{q=1}^k \sum_{t=1}^{|\hat{S}_q^\omega|} \rho_{q,i_{q,t}^\omega}^\omega(\hat{\mathbf{S}}_{q,(t)}^\omega) \xi_{i_{q,t}^\omega}^\omega x_{q,i_{q,t}^\omega} \right) \quad (27c)$$

$$= \Phi_A(\hat{\mathbf{x}}) - \sum_{q=1}^k \sum_{\omega \in \Omega} \sum_{t=1}^{|\hat{S}_q^\omega|} \hat{p}_\omega \rho_{q,i_{q,t}^\omega}^\omega(\hat{\mathbf{S}}_{q,(t)}^\omega) \xi_{i_{q,t}^\omega}^\omega x_{q,i_{q,t}^\omega}. \quad (27d)$$

From the feasibility of $\bar{\mathbf{S}}^\omega$ for given \mathbf{x} , (27a) holds. Inequality (27b) is based on the definition of $\{\bar{p}_\omega\}_{\omega \in \Omega}$. From (26), (27c) and (27d) follow. \blacksquare

Proof of Theorem 7. Given that Ω is a set of finite possible realizations, we solve finite $|\Omega|$ number of subproblems in each iteration of the while loop (steps from line 2 to line 15). For each subproblem (a k -submodular maximization problem), an optimal solution can be found in a finite iterations, given that the ground set $N = \{1, \dots, n\}$ has a finite number of elements (Yu and Küçükyavuz, 2021). Additionally, we solve the master problem (a mixed-binary problem) once and solve distribution separation problem in line 6 and 7) at most nk number of times. Assuming the existence of an algorithm that converges in finite iterations for distribution separation problem (line 6 and 7), the steps from line 2 to line 15 will also take finite number of iterations for any counter L . Now, we only need to prove that steps from line 2 to line 15 iterate finite number of times, i.e., L is finite, until the algorithm converges to an optimal solution. Consider an iteration $L = t < \infty$. Suppose we obtain optimal solution (\mathbf{x}^t, η^t) by solving the master problem \mathcal{M}_{DRR}^t , where $\eta^t = \theta_{dr}^{lb}$. If there is no optimality cut separating (\mathbf{x}^t, η^t) , then this solution is feasible for the DRA k -SIP, implying $\eta^t = \Phi_R(\mathbf{x}^t) = \theta_{dr}^{ub}$. Hence, $\eta^t = \theta_{dr}^{lb} = \theta_{dr}^{ub}$, which satisfies termination condition, and we have optimal solution in the finite iterations (at iteration t).

If there exists an optimality cut separating (\mathbf{x}^t, η^t) , it will be added as in line 11 and the process (while loop) continues. Assume we obtain an optimal master solution (\mathbf{x}^u, η^u) in iteration u where $u > t$. If we already visit \mathbf{x}^u in previous iterations, this implies (\mathbf{x}^u, η^u) is a feasible solution of the DRR k -SIP and no new optimality cut will be added. We already show that in this case, algorithm will be terminated with the optimal solution (\mathbf{x}^u, η^u) . Finally, if (\mathbf{x}^u, η^u) is the new solution we never visited before, the new optimality cut will be added and algorithm will be continued. Since the attacker's solution \mathbf{x} is a vector of binary variables, there exists finite number of feasible attacker's solution that can be visited. Consequently, the algorithm will be terminated in finite iterations with an optimal solution because of Observation 6. \blacksquare

5 Results of Computational Experiments

In this section, we present the computational results for solving DRA k -SIP, DRR k -SIP, risk-neutral (stochastic) k -SIP, and deterministic k -SIP instances. The evaluation is divided into two categories based on the objective function of the defender: $k = 1$ and $k = 2$ submodular function in feature selection interdiction problem (Section 5.1) and weighted coverage interdiction problem (Section 5.2), respectively. The algorithms were implemented in Python 3.8.5 with the Gurobi 9.5.2 optimization solver and the experiments were conducted using Intel Xeon(R) W-2255 processor (3.7 GHz) with 32GB RAM. We consider two types of ambiguity set that are widely used in the literature: Moment matching set and Wasserstein ambiguity set. The moment matching set, denoted by \mathfrak{P}_M , is defined by constraining first moment of the random variables within predetermined lower and upper bounds denoted by l_1 and u_1 , respectively. Let \bar{m}_1 be the first moment of the random variable ξ , i.e., $\bar{m}_1 = \sum_{\omega \in \Omega} \xi^\omega / |\Omega|$. Given a tolerance level ϵ_M , we obtain the bounds as $l_1 = (1 - \epsilon_M)\bar{m}_1$ and $u_1 = (1 + \epsilon_M)\bar{m}_1$. The moment matching set is then defined as:

$$\mathfrak{P}_M := \left\{ \{p_\omega\}_{\omega \in \Omega} : l_1 \leq \sum_{\omega \in \Omega} p_\omega \mathbb{E}(\omega) \leq u_1, \sum_{\omega \in \Omega} p_\omega = 1; p_\omega \geq 0, \forall \omega \in \Omega \right\},$$

where $\mathbb{E}[\cdot]$ is the expectation defined on Ω and its sigma-algebra \mathcal{F} .

In contrast, the Wasserstein ambiguity set is a set of probability distributions within a given $\epsilon_W (> 0)$ distance from a reference distribution $P^* = \{p_\omega^*\}_{\omega \in \Omega}$ and is defined as:

$$\begin{aligned} \mathfrak{P}_W := & \left\{ P = \{p_\omega\}_{\omega \in \Omega} : \sum_{\omega \in \Omega} p_\omega = 1; \sum_{\omega_i \neq \omega_j \in \Omega} \|\omega_i - \omega_j\|_1 v_{\omega_i, \omega_j} \leq \epsilon_W; \right. \\ & \sum_{\omega_j \in \Omega} v_{\omega_i, \omega_j} = p_{\omega_i}, \text{ for all } \omega_i \in \Omega; \sum_{\omega_i \in \Omega} v_{\omega_i, \omega_j} = p_{\omega_j}^*, \forall \omega_j \in \Omega; \\ & \left. p_\omega \geq 0, \text{ for all } \omega \in \Omega; v_{\omega_i, \omega_j} \geq 0, \forall \omega_i, \omega_j \in \Omega \right\}. \end{aligned} \quad (28)$$

5.1 Feature Selection Interdiction Problem

5.1.1 Instance Generation and setting

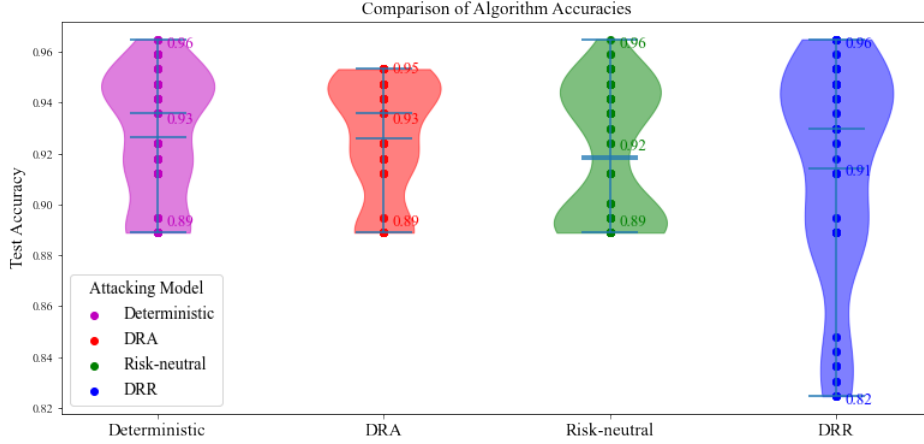
For FSIP instances, we use Wisconsin Breast Cancer Data set (\mathcal{D}), which is widely recognized in the field of medical informatics for research purposes (Wolberg et al., 1995). This data set is available from the UCI Machine Learning Repository (Carrizosa et al., 2008; De Loera et al., 2017) and consists of 569 data points each representing a patient. Each patient is described by $n = 30$ features derived from digitized images of breast mass biopsies. The data set is primarily used for binary classification tasks within machine learning frameworks. We assume that each data point inherently possesses uncertainty, indicating potential noise within each data point. Specifically, the “true” data point exists within a ball of radius $\delta (\geq 0)$ that is centered around each data point in \mathcal{D} .

Utilizing the data set \mathcal{D} , we generated multiple data sets, $\{\mathcal{D}^\omega\}_{\omega \in \Omega}$, to represent a set of distinct possible realizations of the true data. For each data set \mathcal{D}^ω , $\omega \in \Omega$, every feature value of the each observed data in \mathcal{D} was perturbed by adding uniformly distributed random noise within the range defined by $\delta = 0.1$. This means that in \mathcal{D}^ω , $\omega \in \Omega$, all data points are perturbed independently but concurrently based on the original data set \mathcal{D} , ensuring that we generated distinct data sets without cross-combining perturbed data points from different realizations. Furthermore, corresponding to each variant of the data set, we generate sets of binary vectors, $\xi^\omega \in \{0, 1\}^n$, $\omega \in \Omega$, indicating the success of the attack on feature i if $\xi_i^\omega = 1$. These vectors are generated from the Bernoulli distribution with a probability 0.75, meaning $\xi_i^\omega = 1$ with probability 0.75 for $i \in \{1, \dots, n\}$. Finally, we fix the number of scenarios $|\Omega|$ to 100.

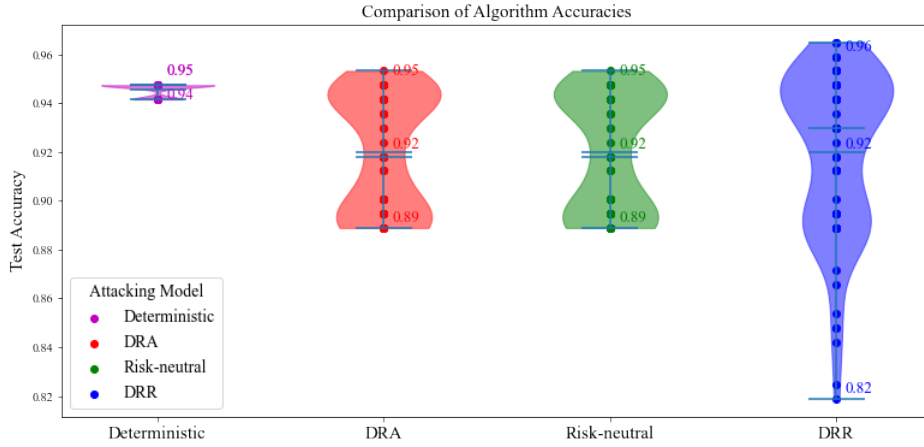
5.1.2 In sample test: Impact of Solutions on Accuracy of SVC Models

Using $\{\mathcal{D}^\omega\}_{\omega \in \Omega}$, we solve DRA, Risk-Neutral and DRR 1-SIP using the proposed decomposition algorithms and obtain optimal solutions for attackers (\mathbf{x}_{RA} , \mathbf{x}_{RN} , \mathbf{x}_{RR}) and for defenders across different data realizations ($\{\mathbf{S}_{RA}^\omega\}_{\omega \in \Omega}$, $\{\mathbf{S}_{RN}^\omega\}_{\omega \in \Omega}$, $\{\mathbf{S}_{RR}^\omega\}_{\omega \in \Omega}$). We also solve the deterministic problem (4) using original data set \mathcal{D} to find an optimal attacker’s solution \mathbf{x}_{DT} . Subsequently, for $\{\mathcal{D}^\omega\}_{\omega \in \Omega}$, we obtained a set of defender’s solution $\{\mathbf{S}_{DT}^\omega\}_{\omega \in \Omega}$ when attacker’s solution is fixed to \mathbf{x}_{DT} . Then, for each scenario $\omega \in \Omega$, we partitioned the data set \mathcal{D}^ω into training and test sets using a 70:30 split. We trained four SVCs using the train data from \mathcal{D}^ω , however, each with defender selected features \mathbf{S}_{DT}^ω , \mathbf{S}_{RA}^ω , \mathbf{S}_{RN}^ω and \mathbf{S}_{RR}^ω respectively. The impact of attacking strategies was assessed by comparing the test accuracy of the SVC models for test data from \mathcal{D}^ω . For the moment matching set with $\epsilon_M = 0.05$, the results are visualized in Figure 2 where each dot represents test accuracy of SVC that is trained with defender selected features under each model setting across all $\omega \in \Omega$. We varied the color based on the problem type and represented the distribution of the accuracy to describe the frequency of the accuracy achieved by the SVCs, highlighting maximum, mean and minimum test accuracy values for each model.

In Figure 2(a), observe that the attacker’s solution \mathbf{x}_{RA} achieves the lowest maximum test accuracy, 95%, among the four evaluated problems, indicating its robustness from the attacker’s perspective, as higher accuracy is undesirable for the attacker. However, this solution could not degrade model performance as significantly as the attacker’s solution \mathbf{x}_{RR} , which can reduce performance to 82% but also paradoxically permits accuracy up to 96% for some realizations. This result aligns with our expectation that attacker would opt for \mathbf{x}_{RR} (distributionally risk-receptive solution) when they aim to minimize the defender’s objective and to reduce test accuracy as much as possible which comes with the risk of allowing the defender to achieve their objective that is not attainable if the attacker opts for any other attacking strategies. In Figure 2(b), we observe outcomes for different budget and notice that by not leveraging the inherent uncertainties present in real-world data sets, \mathbf{x}_{DT} strategy fails to effectively degrade the model’s performance in comparison to the other three attacking strategies. This (deterministic) attacking strategy leads to a relatively stable but less impactful outcome from an attacker’s perspective while the other three (stochastic) attacking solutions force a wider range of model performance, showing their ability to substantially influence model accuracy or compromise data integrity. Overall, from the defender’s per-



(a) Budget 7 and $\epsilon_M = 0.05$



(b) Budget 8 and $\epsilon_M = 0.05$

Figure 2: Performance of Support Vector Classifiers (SVCs) Trained on Defender-Selected Features Across Different Problem Scenarios and Budget Settings

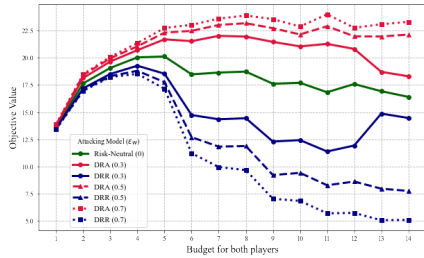
spective, solving the DRR k -SIP offers insights by identifying the most vulnerable features, whose removal could significantly compromise data quality.

In Tables 1 and 2, we report the objective function values, $\Phi_A(\mathbf{x}_{RA})$, $\Phi_N(\mathbf{x}_{RN})$, and $\Phi_R(\mathbf{x}_{RR})$, for instances with same budget for the attacker and defender, ranging from 1 to 14. In Figures 3(a) and 3(b), we present the objective function values as we increase ϵ_W and ϵ_M . Observe that the gap between risk-averse solution values and risk-receptive solution values increase as we increase the ϵ_W and ϵ_M to increase the size of the ambiguity set. Also, objective values from DRA k -SIP and DRR k -SIP establish an interval for the objective value of the Risk-Neutral k -SIP, this trend implies that when the attacker has less information associate with the probability distribution, i.e., when they assume the larger ambiguity set, they construct large confidence interval for the expectation of defender's objective value. For

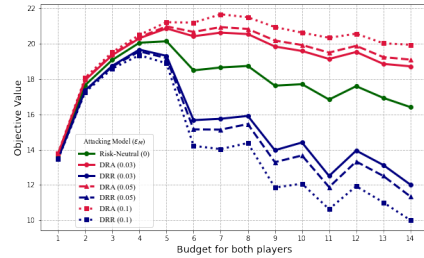
the attacker, the interval constructed for the expected values of the defender’s objective in a distributional ambiguity, as illustrated in Figure 3(a), serves as a valuable reference which enables them to decide whether to pursue aggressive actions or conservative approach.

Instance (Budgets)	Wasserstein ambiguity set (ϵ_W)											
	$\epsilon_W = 0.3$						$\epsilon_W = 0.5$					
	DRA k -SIP		Risk Neutral k -SIP		DRR k -SIP		DRA k -SIP		Risk Neutral k		DRR k -SIP	
	Reward $\Phi_A(\mathbf{x}_{RA})$	Time (s)	Reward $\Phi_N(\mathbf{x}_{RN})$	Time (s)	Reward $\Phi_R(\mathbf{x}_{RR})$	Time (s)	Reward $\Phi_A(\mathbf{x}_{RA})$	Time (s)	Reward $\Phi_N(\mathbf{x}_{RN})$	Time (s)	Reward $\Phi_R(\mathbf{x}_{RR})$	Time (s)
1	13.8	1.4	13.6	1.3	13.5	1.6	13.8	0.8	13.6	1.0	13.5	1.5
2	18.1	39.5	17.6	39.6	17.2	49.7	18.4	46.0	17.6	39.5	17.0	42.8
3	19.7	129.4	19.1	179.6	18.5	172.2	20.0	135.6	19.1	180.1	18.3	179.5
4	20.7	316.8	20.0	423.5	19.3	413.9	21.1	317.6	20.0	422.3	18.8	497.3
5	21.7	912.9	20.1	589.9	18.5	507.2	22.3	983.2	20.1	590.3	17.8	660.3
6	21.5	848.1	18.5	399.0	14.7	845.0	22.5	1799.9	18.5	400.2	12.7	599.8
7	22.0	2016.7	18.6	553.9	14.3	693.7	23.0	2656.4	18.6	552.9	11.8	910.7
8	22.0	2074.5	18.7	1068.6	14.4	1610.4	23.2	3451.3	18.7	1068.2	11.9	1203.5
9	21.5	3376.7	17.6	1609.1	12.3	1497.9	22.7	2639.0	17.6	1618.6	9.2	1338.8
10	21.1	2701.5	17.7	1301.2	12.4	1954.6	22.2	1788.8	17.7	1300.7	9.4	1390.8
11	21.3	2782.0	16.8	1722.2	11.4	2290.5	22.9	3779.9	16.8	1721.8	8.3	1870.5
12	20.8	2684.7	17.6	2103.6	11.9	2321.2	22.0	2696.0	17.6	2093.0	8.6	1927.1
13	18.7	2246.2	16.9	1629.1	14.9	1903.1	22.0	2077.3	16.9	1635.8	7.9	2504.8
14	18.3	4220.5	16.4	2331.7	14.5	2458.4	22.1	3937.3	16.4	2331.8	7.7	2863.2

Table 1: Computational results for solving DRA k -SIP, Risk-neutral k -SIP and DRR k -SIP with Wisconsin Breast Cancer Data with Wasserstein ambiguity set



(a) Comparisons of optimal objective values with Wasserstein ambiguity set defined by $\epsilon_W \in \{0.3, 0.5, 0.7\}$



(b) Comparisons of optimal objective values with Moment matching set defined by $\epsilon_M \in \{0.03, 0.05, 0.1\}$

Figure 3: Comparisons of optimal objective values with different ambiguity sets

5.1.3 Out of Sample Testing of Deterministic, Risk-Neutral, DRA, and DRR

For out-of-sample testing, we generate another set of possible realizations $\hat{\Omega} := \{\hat{\omega}_1, \dots, \hat{\omega}_{|\hat{\Omega}|}\}$ of (ξ, \mathcal{D}) using Bernoulli and uniform distributions for ξ and \mathcal{D} , respectively, as those employed for generating in-sample tests. Then, we mirrored the same procedure used in section 5.1.2 to evaluate the impact of attacking solutions through the test accuracy of SVCs which are trained solely with defender selected features. For these experiments, we increased

Instance (Budgets)	Moment matching set (ϵ_M)											
	$\epsilon_M = 0.03$						$\epsilon_M = 0.05$					
	DRA k -SIP		Risk Neutral k -SIP		DRR k -SIP		DRA k -SIP		Risk Neutral k		DRR k -SIP	
	Reward $\Phi_A(\mathbf{x}_{RA})$	Time (s)	Reward $\Phi_N(\mathbf{x}_{RN})$	Time (s)	Reward $\Phi_R(\mathbf{x}_{RR})$	Time (s)	Reward $\Phi_A(\mathbf{x}_{RA})$	Time (s)	Reward $\Phi_N(\mathbf{x}_{RN})$	Time (s)	Reward $\Phi_R(\mathbf{x}_{RR})$	Time (s)
1	13.8	3.6	13.6	1.0	13.5	54.2	13.8	3.4	13.6	1.1	13.5	51.1
2	17.9	36.0	17.6	39.3	17.4	115.4	18.0	35.7	17.6	38.8	17.3	122.6
3	19.3	158.1	19.1	179.3	18.7	304.3	19.4	156.7	19.1	178.2	18.7	298.0
4	20.3	364.1	20.0	425.2	19.7	775.1	20.4	386.4	20.0	419.8	19.6	750.7
5	20.9	795.4	20.1	593.0	19.3	802.8	21.0	928.7	20.1	587.9	19.2	812.3
6	20.4	927.8	18.5	407.7	15.7	624.6	20.7	1193.4	18.5	397.3	15.1	613.2
7	20.6	1567.9	18.6	552.4	15.7	747.2	20.9	1528.9	18.6	552.0	15.1	657.5
8	20.5	1216.4	18.7	1067.8	15.9	1264.5	20.8	2555.8	18.7	1065.9	15.4	1286.3
9	19.8	2048.0	17.6	1605.8	14.0	2031.9	20.2	2078.5	17.6	1605.7	13.3	1656.0
10	19.6	1744.1	17.7	1302.2	14.4	1953.2	19.9	1827.8	17.7	1303.6	13.7	2029.1
11	19.1	2832.8	16.8	1724.6	12.5	2273.5	19.5	3051.6	16.8	1710.0	11.9	2586.1
12	19.5	2723.9	17.6	2077.2	13.9	2353.0	19.9	3765.9	17.6	2067.2	13.3	2373.3
13	18.8	2195.8	16.9	1641.7	13.1	2736.8	19.2	2203.9	16.9	1674.9	12.5	4221.1
14	18.7	2235.5	16.4	2335.0	12.0	3864.4	19.1	1586.1	16.4	2413.6	11.4	4650.6

Table 2: Computational results for solving DRA k -SIP, Risk-neutral k -SIP and DRR k -SIP with Wisconsin Breast Cancer Data with Moment matching set

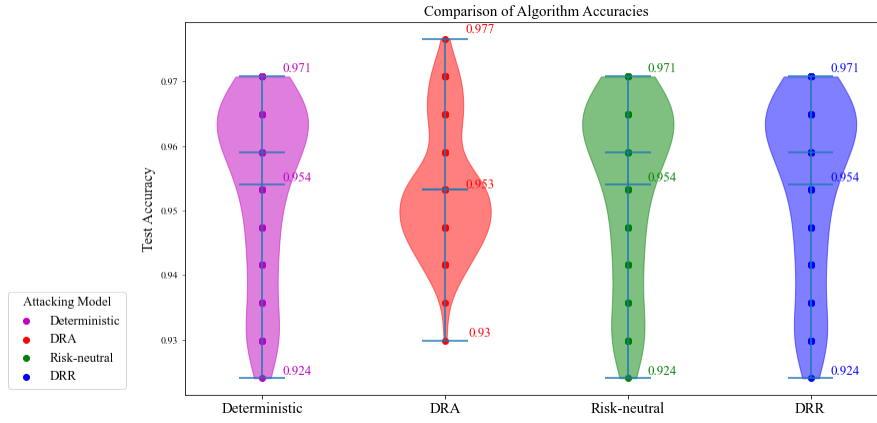
the number of scenarios to 300, i.e., $|\hat{\Omega}| = 300$. We varied the size of the Wasserstein ambiguity set and for each defined ambiguity set, we followed the aforementioned procedure across different budget settings for both the attacker and the defender. The test results are presented in Figures 4, 5 and 6.

Overall, we notice that the solution obtained using the stochastic models, \mathbf{x}_{RA} and \mathbf{x}_{RR} provide significant advantages over \mathbf{x}_{DT} obtained by solving deterministic model. The \mathbf{x}_{RA} reduces the variability of the outcome, offering a robust attacking strategy that minimizes the risk. Also, \mathbf{x}_{RR} degrades the model performance more effectively than \mathbf{x}_{DT} , presenting a more aggressive strategy. These two distinct strategies offer decision makers the flexibility to choose between robustness and aggressiveness.

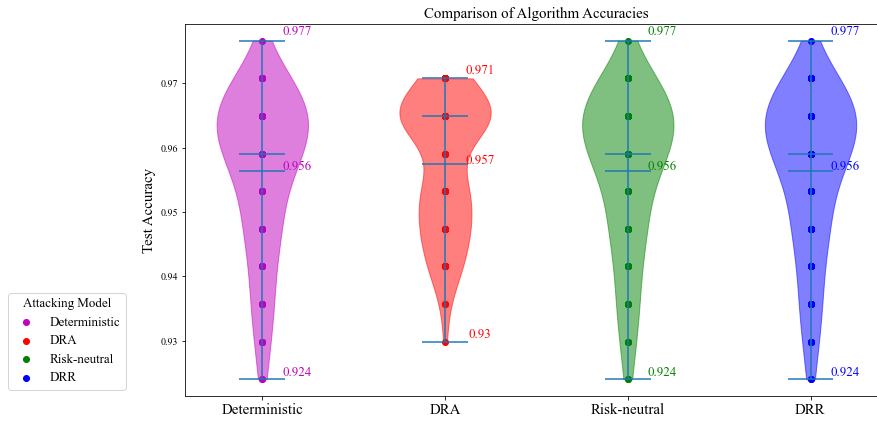
5.2 Weighted Coverage Interdiction Problem

5.2.1 Instance Generation

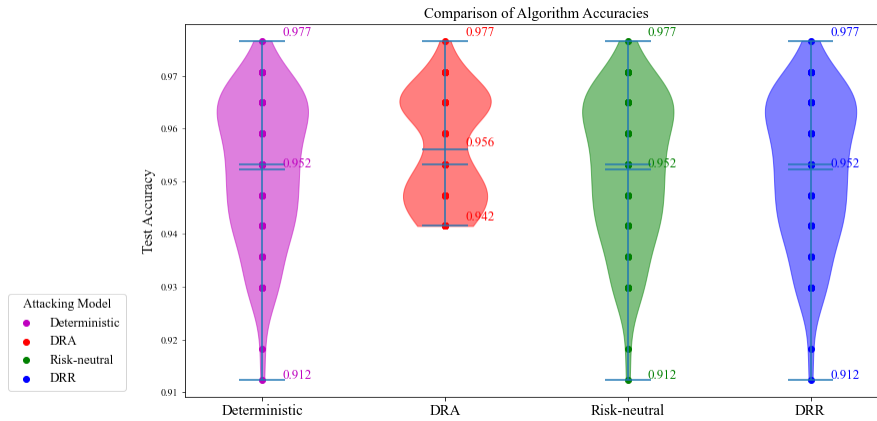
For $k = 1$, we use instances provided by Tanınmış and Sinnl (2022) for problem presented in subsection 3.2.2, where customer locations are randomly generated from Uniform $[1, 10] \times [1, 10]$ and candidate locations for the sensor is same as the generated location of the customers. For customer $j \in N$, we randomly generate associated reward p_j from Uniform $[1, 100]$ and the customer j is covered by sensor placed at location $i \in N$ if euclidean distance $d_{ij} \leq r$ where r denotes the radius of the sensor. Instances were created for radii $r = \{1, 2\}$, maintaining uniform sensor radius within each instance. For $k = 2$, indicating the presence of two sensor types with distinct radii ($r = 1$ or $r = 2$), it is possible to install both types simultaneously. Sensors with a larger radius ($r = 2$), although offering a wider coverage range, yield only half the reward per customer compared to those with a radius of $r = 1$. For both categories, i.e., $k = 1$ and $k = 2$, we generate a realization $\xi^\omega \in \{0, 1\}^n$, $\omega \in \Omega$,



(a) $\epsilon_W = 0.7$

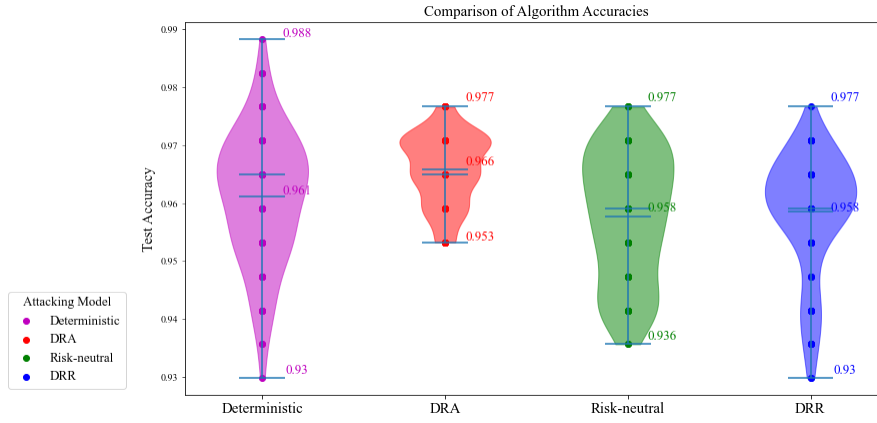


(b) $\epsilon_W = 1$

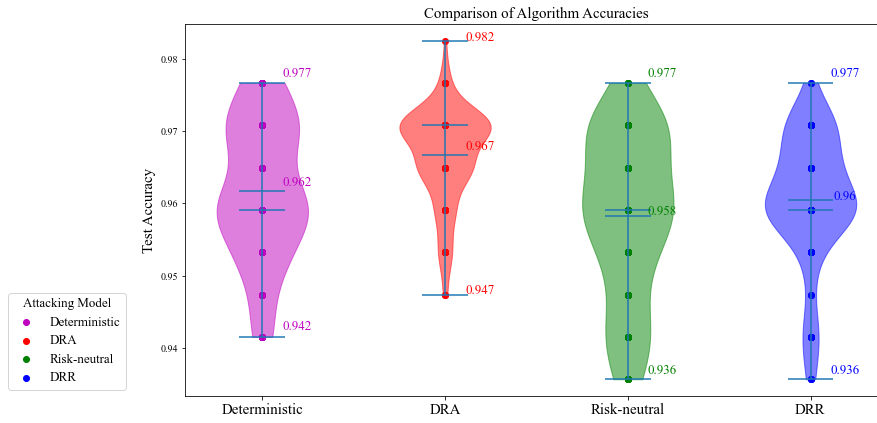


(c) $\epsilon_W = 1.5$

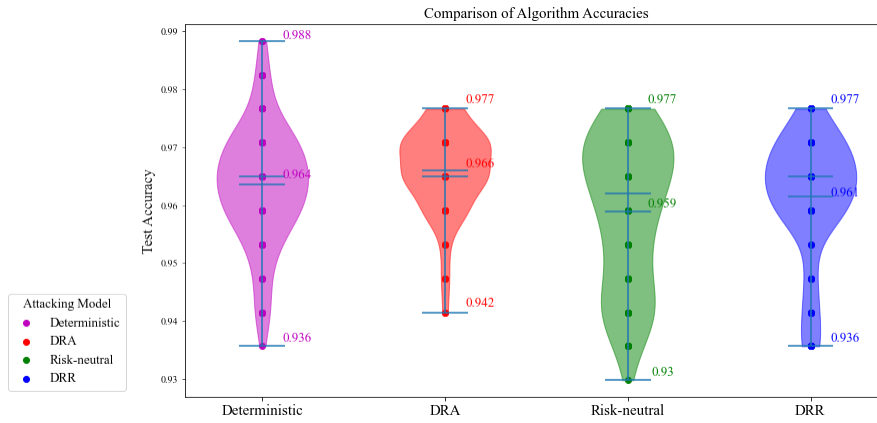
Figure 4: Performance of Support Vector Classifiers (SVCs) trained on defender selected features across different problem scenarios with varying ϵ_W and fixed attacker and defender budget of 6.



(a) $\epsilon_W = 0.7$

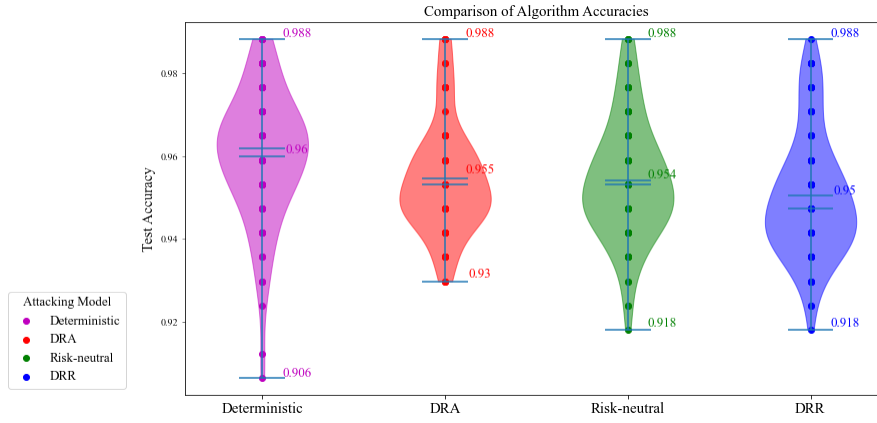


(b) $\epsilon_W = 1$

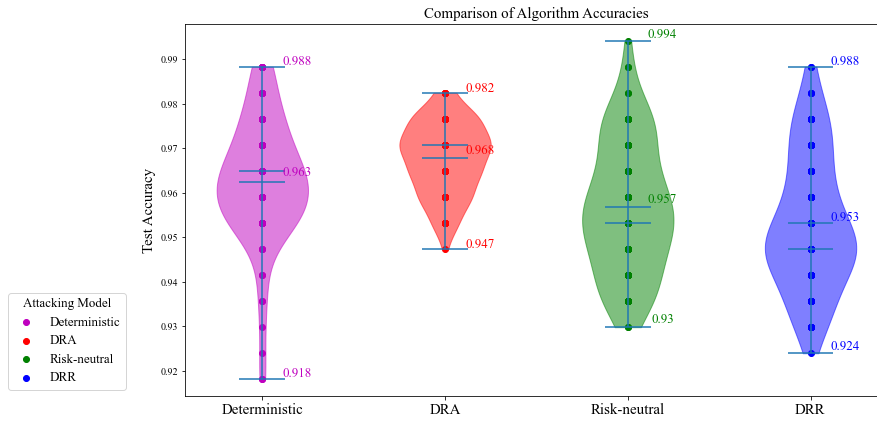


(c) $\epsilon_W = 1.5$

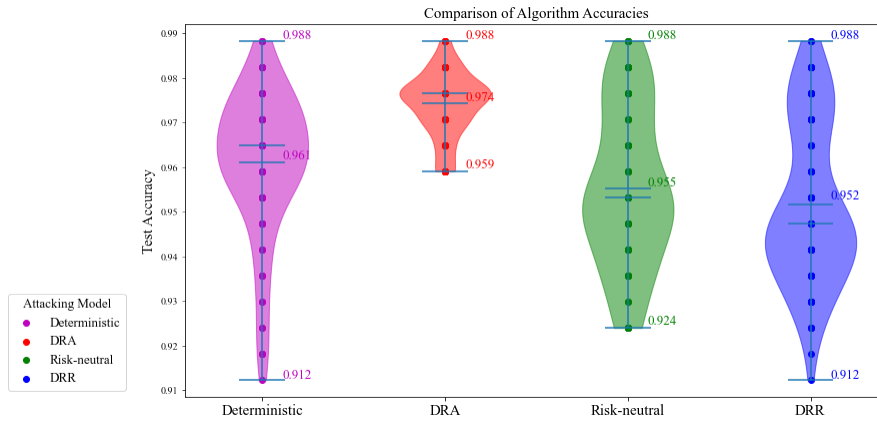
Figure 5: Performance of Support Vector Classifiers (SVCs) trained on defender selected features across different problem scenarios with varying ϵ_W and fixed attacker and defender budget of 7.



(a) $\epsilon_W = 0.7$



(b) $\epsilon_W = 1$



(c) $\epsilon_W = 1.5$

Figure 6: Performance of Support Vector Classifiers (SVCs) trained on defender selected features across different problem scenarios with varying ϵ_W and fixed attacker and defender budget of 14.

n	$ \Omega $	Deterministic k -SIP		DRA k -SIP		Risk-Neutral k -SIP		DRR k -SIP	
		Reward $\Phi_D(\mathbf{x}_{DT})$	Time (s)	Reward $\Phi_A(\mathbf{x}_{RA})$	Time (s)	Reward $\Phi_N(\mathbf{x}_{RN})$	Time (s)	Reward $\Phi_R(\mathbf{x}_{RR})$	Time (s)
50	100	1687	0.37	1,770	21	1,748	10	1,722	56
60		2093	0.57	2,215	67	2,185	38	2,147	252
70		2597	1.2	2,717	361	2,690	204	2,655	1,370
80		3044	2.8	3,194	2,378	3,164	993	3,123	4,610
90		3599	11	3,773	5,722	3,733	2,602	3,703	14,690
100		2925	37	3,133	6,933	3,100	3,906	3,034	16,815

Table 3: Weighted Coverage Interdiction Problem: Computational results for solving Deterministic k -SIP, DRA k -SIP, Risk-Neutral k -SIP and DRR k -SIP where $k = 1$.

following a Bernoulli distribution with a success probability of 0.75.

5.2.2 Computational Results

Table 3 details the results from solving Deterministic k -SIP and applying our decomposition methods to solve DRA k -SIP, Risk-Neutral k -SIP and DRR k -SIP, with columns for “Reward” and “Time (s)” indicating the objective values and computational times, respectively. We report average over 18 instances for each row in Table 3, except for $n = 100$, where the results are averaged over 8 instances. For each n , we assume that budget for the attacker and defender is $0.1 \times n$. As expected, defender’s covered rewards for DRR k -SIP are consistently less than those for Risk-Neutral k -SIP and DRA k -SIP. This suggests that DRR k -SIP could serve as a strategic tool for attackers who are willing to take a risk, providing them with a quantitative measure of how much they can potentially diminish the defender’s objective of covered demand. From the vulnerability analysis standpoint for the defender, the DRR k -SIP identifies the most severe attacking strategies, enabling the identification of critical locations, which can significantly reduce captured reward if compromised. This solution allows the defender to plan fortification of locations against potential attacks obtained from DRR k -SIP. This approach is reasonable, as defenders cannot anticipate the risk preferences of attackers, requiring them to prepare for a risk-receptive attackers as well. Conversely, for attackers who prefer to avoid a risk, the DRA k -SIP offers a conservative estimate of the maximum reward the defender could achieve, thereby informing a risk-averse strategy. Note that defender’s $\Phi_D(\mathbf{x}_{DT})$ are less than those of the other three problems, reflecting the naive assumption in the deterministic problem that all attacks are successful. This assumption, although optimistic from the attacker’s perspective, does not realistically capture the uncertain nature of real-world scenarios, potentially misleading the attacker in determining the best attacking solution.

To underscore the importance of accounting for uncertainty in the optimization models, we measure Value of Stochastic Solution (VSS) that is computed as follows.

$$\text{VSS} = \Phi_N(\mathbf{x}_{DT}) - \Phi_N(\mathbf{x}_{RN}),$$

where $\Phi_N(\mathbf{x}_{DT})$ returns the defender’s expected covered reward when attacker’s adheres to \mathbf{x}_{DT} (deterministic optimal solution) and there is no distributional ambiguity. Additionally,

n	$\Phi_N(\mathbf{x}_{DT})$	$\Phi_N(\mathbf{x}_{RN})$	VSS	# of instances VSS>0	$\Phi_A(\mathbf{x}_{DT})$	$\Phi_A(\mathbf{x}_{RA})$	VAS	# of instances VAS>0	$\Phi_R(\mathbf{x}_{DT})$	$\Phi_R(\mathbf{x}_{RR})$	VRS	# of instances VRS>0
50	1760.7	1748.0	25.3	9	1787.6	1770.5	25.7	12	1732.2	1722.7	21.5	8
60	2197.5	2185.5	19.6	11	2234.0	2215.4	24.0	14	2158.0	2147.9	20.1	9
70	2707.1	2690.2	20.3	15	2740.1	2717.2	24.2	17	2671.8	2655.6	19.5	15
80	3182	3164.5	23.2	14	3220.0	3194.6	35.1	13	3138.8	3123.7	20.8	13
90	3770.5	3743.1	30.9	16	3806.5	3773.2	49.9	12	3723.5	3703.8	32.4	11
100	3156.8	3100.7	64.0	7	3330.5	3133.4	197.5	8	3038.1	3034.0	32.5	1

Table 4: Average values of VSS, VAS and VRS

we introduce Value of Distributionally Risk Averse Solution (VAS) and Value of Distributionally Risk Receptive Solution (VRS) as follows.

$$\text{VAS} = \Phi_A(\mathbf{x}_{DT}) - \Phi_A(\mathbf{x}_{RA}) \text{ and } \text{VRS} = \Phi_R(\mathbf{x}_{DT}) - \Phi_R(\mathbf{x}_{RR}),$$

By definition, VSS, VAS and VRS are non-negative as \mathbf{x}_{RN} , \mathbf{x}_{RA} and \mathbf{x}_{RR} are all optimal solutions and \mathbf{x}_{DT} is a feasible solution. In Table 4, we report average of VSS only for instances where $\text{VSS} > 0$, out of 18 instances for each n , except for $n = 100$, and similarly, average VAS and VRS are reported for instances where $\text{VAS} > 0$ and $\text{VRS} > 0$.

From Table 4, we notice that VSS, VAS and VRS increase as n increase. For $n = 100$, VAS is 197.5 and this suggests that if the attacker naively relies on the deterministic optimal solution \mathbf{x}_{DT} despite the presence of uncertainty, they miss the opportunity to diminish the defender’s reward by 197.5 units, which could have been achieved by solving DRA k -SIP and opting \mathbf{x}_{RA} . This interpretation holds when VSS or VRS is greater than zero.

As indicated in Figure 7, VAS consistently exceeds both VSS and VRS for all $n \in \{50, 60, 70, 80, 90, 100\}$ and interestingly, as n increases, the value of all measures, VAS, VSS and VRS, also increases. In other words, as the number of candidate locations and the budgets for both decision-makers increase, the advantages, an attacker could gain by opting for stochastic decisions, \mathbf{x}_{RA} , \mathbf{x}_{RN} and \mathbf{x}_{RR} , also increase.

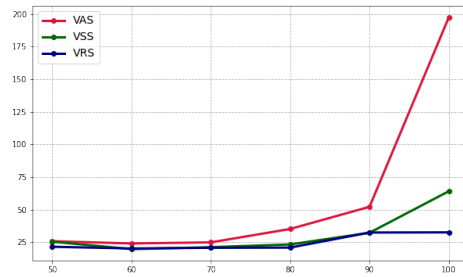


Figure 7: Comparison of VSS, VAS and VRS

Weighted Coverage Interdiction Problem with $k = 2$. Table 5 details the results for bi-submodular function. The results are averaged over 10 instances for each row in Table 3, and for each n , we assume that budget for the attacker and defender is $0.1 \times n$. Additionally, we set the number of scenarios $|\Omega| = 30$. We observe that defender’s optimal captured rewards for DRR 2-SIP is less than those of Risk-neutral 2-SIP and DRA 2-SIP. Again, this results aligns with the fact that DRR k -SIP provides the solution where the attacker can degrade the defender’s objective to the greatest extent, making it useful for vulnerability analysis from the defender’s perspective. Conversely, the defender’s capture rewards for DRA 2-SIP are greater than those of Risk-neutral 2-SIP and DRR 2-SIP, as it provides the conservative strategy towards the distributional ambiguity for the attacker.

n	$ \Omega $	Deterministic k -SIP		DRA k -SIP		Risk-Neutral k -SIP		DRR k -SIP	
		Reward $\Phi_D(\mathbf{x}_{DT})$	Time (s)	Reward $\Phi_A(\mathbf{x}_{RA})$	Time (s)	Reward $\Phi_N(\mathbf{x}_{RN})$	Time (s)	Reward $\Phi_R(\mathbf{x}_{RR})$	Time (s)
10		83.0	0.09	84.6	0.1	84.4	0.1	84.2	0.2
20		310	0.2	323	1.3	321	1.4	318	1.5
30		730	0.7	842	8.8	823	8.6	802	14
40	30	933	6.2	1,045	76	1,030	85	1,014	129
50		1,278	9.5	1,452	142	1,428	150	1,408	238
60		2,013	2,550	2,160	7,053	2,142	8,884	2,124	16,870
70		2,732	1,425	2,963	4,341	2,932	5,033	2,898	10,490

Table 5: Weighted Coverage Interdiction Problem: Computational results for solving Deterministic k -SIP, DRA k -SIP, Risk-Neutral k -SIP and DRR k -SIP where $k = 2$.

6 Conclusion

To address submodular optimization in adversarial and uncertain environment, we introduced Distributionally Risk-Averse k -Submodular Interdiction Problem (DRA k -SIP) and Distributionally Risk-Receptive k -Submodular Interdiction Problem (DRR k -SIP) and presented exact solution approaches for them. We conducted computational experiments on instances of Feature Selection Interdiction Problem (FSIP) and Multi-type Sensor Coverage Interdiction Problem. Note that feature selection is a key concept in machine learning, underscoring the importance of these results for practical applications. We analyzed the solutions obtained from both problems from each of the decision maker’s perspective with varying levels of risk-appetite. In FSIP, the optimal solution from DRA 1-SIP demonstrated robust feature removal strategy which is effective from the attacker’s risk-averse (or conservative) perspective. Conversely, solution from DRR 1-SIP identified critical features whose removal reduce the quality of data the most from the attacker’s risk-receptive (or defender’s risk-averse) perspective. In general, the DRA k -SIP seeks to determine the optimal expected value of the defender’s objective function under the worst probability distribution from the attacker’s perspective, providing a robust strategy suitable for risk-averse attackers. In contrast, the DRR k -SIP offers insights into effective strategies for risk-taking attackers, thereby identifying critical vulnerabilities in the defender’s system.

Data Availability Statement The instances used for computational studies in this paper will be made available in “Submodular-Interdiction-Game” folder at <https://github.com/Bansal-ORGroup/>.

References

Boykov, Y. Y. and Jolly, M.-P. (2001). Interactive graph cuts for optimal boundary & region segmentation of objects in nd images. In *IEEE international conference on computer vision. ICCV 2001*, volume 1, pages 105–112. IEEE.

- Carrizosa, E., Martin-Barragan, B., and Morales, D. R. (2008). Multi-group support vector machines with measurement costs: A biobjective approach. *Discrete Applied Mathematics*, 156(6):950–966.
- Dai, H., Li, H., Tian, T., Huang, X., Wang, L., Zhu, J., and Song, L. (2018). Adversarial attack on graph structured data. In *International Conference on Machine Learning (ICML)*, pages 1115–1124. PMLR.
- De Loera, J. A., Haddock, J., and Needell, D. (2017). A sampling kaczmarz–motzkin algorithm for linear feasibility. *SIAM Journal on Scientific Computing*, 39(5):S66–S87.
- Dekel, O. and Shamir, O. (2008). Learning to classify with missing and corrupted features. In *International Conference on Machine Learning (ICML)*, pages 216–223.
- Dupačová, J. (1987). The minimax approach to stochastic programming and an illustrative application. *Stochastics: An International Journal of Probability and Stochastic Processes*, 20(1):73–88.
- Fulkerson, D. R. and Harding, G. C. (1977). Maximizing the minimum source-sink path subject to a budget constraint. *Mathematical Programming*, 13(1):116–118.
- Globerson, A. and Roweis, S. (2006). Nightmare at test time: robust learning by feature deletion. In *International Conference on Machine Learning (ICML)*, pages 353–360.
- Goodfellow, I. J., Shlens, J., and Szegedy, C. (2014). Explaining and harnessing adversarial examples. *arXiv preprint arXiv:1412.6572*.
- He, Z., Rakin, A. S., and Fan, D. (2019). Parametric noise injection: Trainable randomness to improve deep neural network robustness against adversarial attack. In *Proceedings of the IEEE/CVF Conference on Computer Vision and Pattern Recognition*, pages 588–597.
- Huber, A. and Kolmogorov, V. (2012). Towards minimizing k-submodular functions. In *Combinatorial Optimization: Second International Symposium, ISCO 2012, Athens, Greece, April 19-21, 2012, Revised Selected Papers 2*, pages 451–462. Springer.
- Israeli, E. and Wood, R. K. (1999). *System interdiction and defense*. PhD thesis, Citeseer.
- Israeli, E. and Wood, R. K. (2002). Shortest-path network interdiction. *Networks: An International Journal*, 40(2):97–111.
- Kang, S. and Bansal, M. (2023). Distributionally risk-receptive and risk-averse network interdiction problems with general ambiguity set. *Networks*, 81(1):3–22.
- Kempe, D., Kleinberg, J., and Tardos, É. (2003). Maximizing the spread of influence through a social network. In *ACM SIGKDD International Conference on Knowledge Discovery and Data mining*, pages 137–146.
- Kothawade, S., Kaushal, V., Ramakrishnan, G., Bilmes, J., and Iyer, R. (2022). Prism: A rich class of parameterized submodular information measures for guided data subset selection. In *AAAI Conference on Artificial Intelligence*, volume 36, pages 10238–10246.

- Krause, A. and Golovin, D. (2014). Submodular function maximization. *Tractability*, 3(71-104):3.
- Krause, A., Leskovec, J., Guestrin, C., VanBriesen, J., and Faloutsos, C. (2008a). Efficient sensor placement optimization for securing large water distribution networks. *Journal of Water Resources Planning and Management*, 134(6):516–526.
- Krause, A., McMahan, H. B., Guestrin, C., and Gupta, A. (2008b). Robust submodular observation selection. *Journal of Machine Learning Research*, 9(12).
- Krause, A., Singh, A., and Guestrin, C. (2008c). Near-optimal sensor placements in gaussian processes: Theory, efficient algorithms and empirical studies. *Journal of Machine Learning Research*, 9(2).
- Kurakin, A., Goodfellow, I., and Bengio, S. (2016). Adversarial machine learning at scale. *arXiv preprint arXiv:1611.01236*.
- Li, Y., Li, T., and Liu, H. (2017). Recent advances in feature selection and its applications. *Knowledge and Information Systems*, 53:551–577.
- Lin, H. and Bilmes, J. (2010). Multi-document summarization via budgeted maximization of submodular functions. In *Human Language Technologies: The 2010 Annual Conference of the North American Chapter of the Association for Computational Linguistics*, pages 912–920.
- Lin, H. and Bilmes, J. A. (2009). How to select a good training-data subset for transcription: submodular active selection for sequences. In *Interspeech*, pages 2859–2862.
- Liu, Y., Wei, K., Kirchhoff, K., Song, Y., and Bilmes, J. (2013). Submodular feature selection for high-dimensional acoustic score spaces. In *2013 IEEE International Conference on Acoustics, Speech and Signal Processing*, pages 7184–7188. IEEE.
- Nemhauser, G. L. and Wolsey, L. A. (1981). Maximizing submodular set functions: formulations and analysis of algorithms. In *North-Holland Mathematics Studies*, volume 59, pages 279–301. Elsevier.
- Nemhauser, G. L., Wolsey, L. A., and Fisher, M. L. (1978). An analysis of approximations for maximizing submodular set functions—i. *Mathematical Programming*, 14:265–294.
- Ohsaka, N. and Yoshida, Y. (2015). Monotone k -submodular function maximization with size constraints. *Advances in Neural Information Processing Systems*, 28.
- Park, S. and Bansal, M. (2024). Algorithms for cameras view-frame placement problems in the presence of an adversary and distributional ambiguity. *IEEE Transactions on Automation Science and Engineering*.
- Qian, C., Shi, J.-C., Tang, K., and Zhou, Z.-H. (2017). Constrained monotone k -submodular function maximization using multiobjective evolutionary algorithms with theoretical guarantee. *IEEE Transactions on Evolutionary Computation*, 22(4):595–608.

- Rafey, A. and Yoshida, Y. (2020). Fast and private submodular and k -submodular functions maximization with matroid constraints. In *International Conference on Machine Learning (ICML)*, pages 7887–7897. PMLR.
- Sakaue, S. (2017). On maximizing a monotone k -submodular function subject to a matroid constraint. *Discrete Optimization*, 23:105–113.
- Scarf, H. E., Arrow, K., and Karlin, S. (1957). *A min-max solution of an inventory problem*. Rand Corporation Santa Monica.
- Singh, A., Guillory, A., and Bilmes, J. (2012). On bisubmodular maximization. In *Artificial Intelligence and Statistics*, pages 1055–1063. PMLR.
- Smith, J. C. and Song, Y. (2020). A survey of network interdiction models and algorithms. *European Journal of Operational Research*, 283(3):797–811.
- Tang, Z., Wang, C., and Chan, H. (2022). On maximizing a monotone k -submodular function under a knapsack constraint. *Operations Research Letters*, 50(1):28–31.
- Tanınmış, K. and Sinnl, M. (2022). A branch-and-cut algorithm for submodular interdiction games. *INFORMS Journal on Computing*, 34(5):2634–2657.
- Vohra, R. V. and Hall, N. G. (1993). A probabilistic analysis of the maximal covering location problem. *Discrete Applied Mathematics*, 43(2):175–183.
- Wei, K., Iyer, R., and Bilmes, J. (2015). Submodularity in data subset selection and active learning. In *International Conference on Machine Learning (ICML)*, pages 1954–1963. PMLR.
- Wolberg, W., Mangasarian, O., Street, N., and Street, W. (1995). Breast Cancer Wisconsin (Diagnostic). UCI Machine Learning Repository. DOI: <https://doi.org/10.24432/C5DW2B>.
- Wollmer, R. (1964). Removing arcs from a network. *Operations Research*, 12(6):934–940.
- Xu, K., Chen, H., Liu, S., Chen, P.-Y., Weng, T.-W., Hong, M., and Lin, X. (2019). Topology attack and defense for graph neural networks: An optimization perspective. *arXiv preprint arXiv:1906.04214*.
- Yu, Q. and Küçükyavuz, S. (2021). An exact cutting plane method for k -submodular function maximization. *Discrete Optimization*, 42:100670.